ACS OMEGA

Open Access

This article is licensed under CC-BY-NC-ND 4.0

http://pubs.acs.org/journal/acsodf

Article

Synthesis, Formation Mechanisms, and Molecular Dynamics Simulation of Novel Benzothiazole and Benzo[1,4]oxazin-3(4*H*)-one as Potential Acetylcholinesterase Inhibitors

Du Duc Nguyen, Dat Van Nguyen, Hue Van Nguyen, Giang Huong Thi Vu, Ha Xuan Nguyen, Hai Hong Thi Le, Dien Huu Pham, Trang Ha Thi Nguyen, Tai Minh Trinh, Nga Thuy Nguyen, Hue Minh Thi Nguyen, and Hoan Quoc Duong*

Cite This: *ACS Omega* 2025, 10, 10835−10851

Read Online

ACCESS | Metrics & More | Article Recommendations | Supporting Information

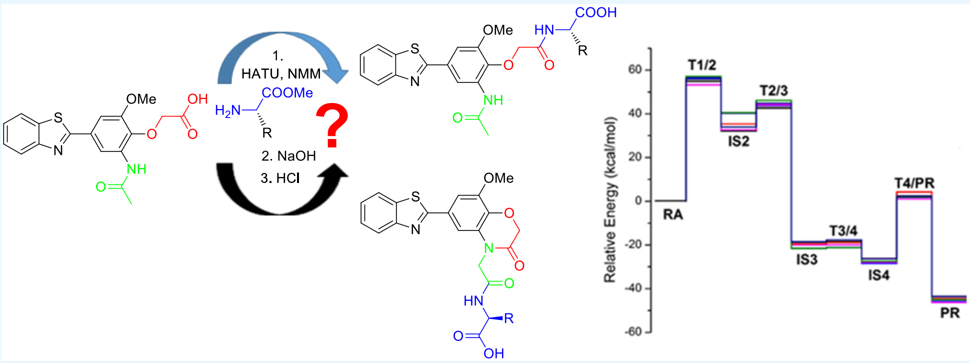

ABSTRACT: A novel series of benzothiazole derivatives was synthesized using straightforward and easily implementable procedures, achieving a high yield. Among these synthesized compounds, amino acids containing the benzothiazole moiety were successfully produced through an 8-step process, with yields reaching as high as 95%. Notably, a serendipitous compound containing both benzothiazole and benzo[1,4]oxazin-3(4*H*)-one moieties was also synthesized using the same protocol, bypassing purification at step 7 and proceeding directly to hydrolysis. This highlights the unique role of the coupling reagent HATU (hexafluorophosphate azabenzotriazole tetramethyluronium) in the reaction, as it facilitated high yields, reaching up to 90%. The structures of the newly synthesized compounds were confirmed through spectral analysis. Density functional theory calculations suggested that energy barriers can be overcome by utilizing the energy from an exothermic reaction, enabling the thermodynamically favorable formation of this novel structure. Compounds **6d** and **6f** demonstrated significant inhibitory activity against the enzyme acetylcholinesterase, with IC_{50} values of 32.00 and 25.33 μg/mL, respectively. Molecular docking and molecular dynamics analyses indicate that compounds **6d** and **6f** hold potential for combating Alzheimer's disease, due to their interactions with critical amino acid residues and structural stability.

INTRODUCTION

Benzothiazole derivatives are aromatic bicyclic compounds containing fused phenyl and thiazole rings. This ring system is frequently found in marine organisms and in natural plant products. For instance, compound **A**, known as Phortress, has demonstrated activity against breast tumors, regardless of estrogen receptor status, as well as against ovarian, renal, lung, and colon cancer cells.[1] Growing interest in the study and synthesis of benzothiazole derivatives stems from their intriguing pharmacological properties, including anti-inflammatory;[2] antibacterial;[3] antiviral;[4] antioxidant;[5] and immunomodulatory effects.[6]

Many significant drugs and therapeutic strategies have been developed, including noninvasive diagnostics for Alzheimer's disease (AD).[7,8] For example, compound **B** demonstrates strong antituberculosis activity, closely approaching that of the reference standard rifampin.[9,10] Additionally, benzothiazole derivatives have contributed to antimalarial drugs.[11] Compound **C** has shown a sugar-lowering activity profile comparable to that of the standard drug glibenclamide, achieving 78% of glucose reduction over control.[12] Furthermore, benzothiazole derivatives are essential substrates in

Received: July 22, 2024
Revised: February 26, 2025
Accepted: March 4, 2025
Published: March 10, 2025

© 2025 The Authors. Published by American Chemical Society

https://doi.org/10.1021/acsomega.4c06760
ACS Omega 2025, 10, 10835−10851

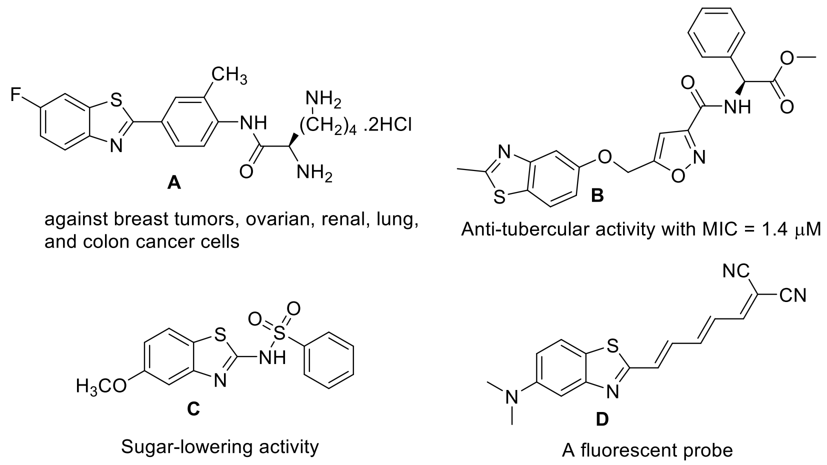

Figure 1. Structures of some benzothiazole derivatives **A**, **B**, **C**, and **D**.

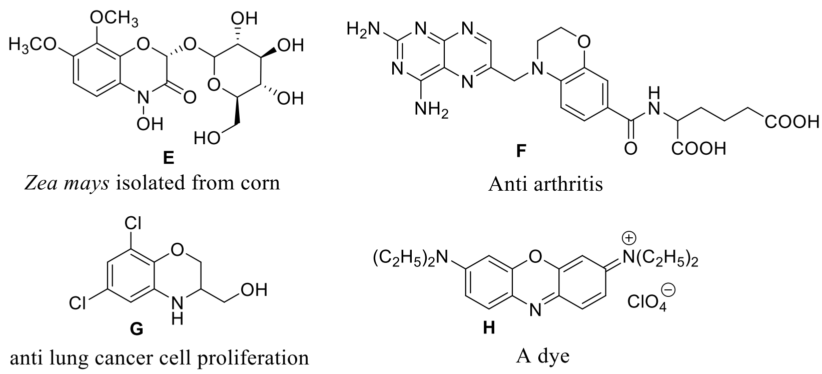

Figure 2. Structures of some benzoxazine and benzo[1,4]oxazin-3(4*H*)-one derivatives **E**, **F**, **G**, and **H**.

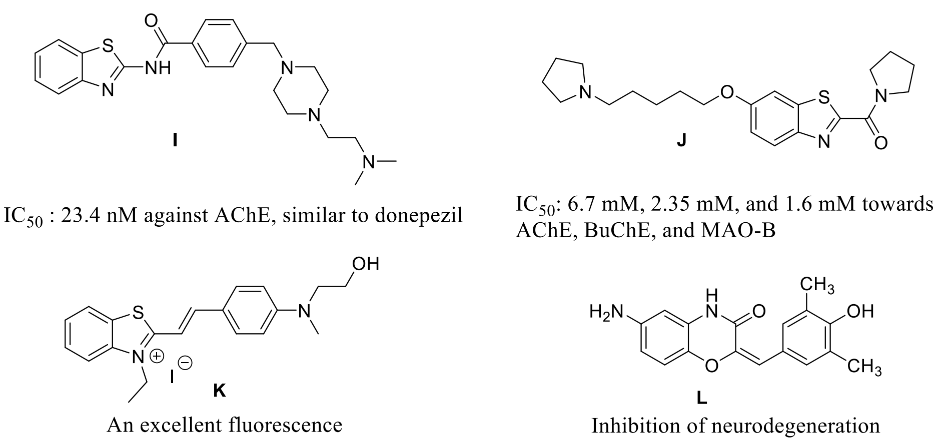

Figure 3. Structures of some benzothiazole and benzoxazine derivatives **I**, **J**, **K**, **L** that have therapeutic effects in the treatment of AD.

fluorescent probes used as sensors for ions and metal cations. For instance, compound **D** is a promising fluorescent probe for detecting of A*β* and *α*-synuclein aggregates in human brain sections,[13,14] Figure 1.

Similarly, benzoxazine derivatives are crucial bicyclic structures found in numerous natural compounds[15−17] as well as in various pharmaceuticals and therapeutic applications. For instance, compound **E** has been isolated from *Zea mays* (a type of corn). Additionally, compound **F** has shown dose-dependent antiarthritic effect, suppressing arthritis progression at doses ranging from 0.5 to 2.5 mg/kg (po).[18] Benzoxazine derivatives also include antioxidant compounds offering neuroprotection,[19] while compound **G** has demonstrated strong efficacy as a small molecule in promoting apoptosis in human umbilical vein endothelial cells and inhibiting lung cancer cell proliferation.[20] Furthermore, benzoxazine-based derivatives serve as antihypertensive agents[21] and as valuable additives in natural products, contributing to glycoside formation in cereal plants.[17] They also support plant resistance to insects, pests, fungi, and other microbial diseases.[22] Additionally, these derivatives can function as materials such as polymer-supported synthons[23] and dyes. For example, compound **H** is a commonly used dye, noted for its high water solubility,[24] Figure 2.

https://doi.org/10.1021/acsomega.4c06760
ACS Omega 2025, 10, 10835−10851

AD is a neurodegenerative disorder characterized by a gradual and progressively worsening decline in memory, cognition, and behavior.[25] Several therapeutic hypotheses have been proposed, including cholinesterase inhibition, amyloid protein formation inhibition, and tau protein accumulation inhibition.[26] Numerous studies based on these hypotheses have led to the Food and Drug Administration (FDA)-approved drugs currently in clinical trials such as donepezil, rivastigmine, and galantamine. However, these drugs only alleviate symptoms and cannot halt disease progression.[27] Consequently, research continues to explore more effective alternatives. Various studies have shown that benzothiazole derivatives exhibit inhibitory activity against acetylcholinesterase (AChE), butyrylcholinesterase (BChE), monoamine oxidase A (MAO-A), and monoamine oxidase B (MAO-B) at low concentrations, suggesting their potential as substitutes for donepezil in AD treatment. For example, compound **I** shows its strongest activity at a concentration of 23.4 ± 1.1 nM against AChE, comparable to donepezil, indicating its potential as a replacement; compound **J** demonstrates therapeutic potential for AD with IC_{50} values of 6.7, 2.35, and 1.6 mM against AChE, BChE, and MAO-B, respectively.[27−29] Additionally, the benzothiazole scaffold shows promise for designing fluorescent probes for selectively detecting A*β* aggregates in AD as demonstrated by compound **K**, which exhibits strong fluorescence with an emission maximum above 598 nm upon binding to A*β* aggregates.[30] Besides the benzothiazole scaffold, benzoxazine derivatives have also shown potential in preventing neurodegenerative diseases, which may support AD treatment. Compound **L** has demonstrated a neuroprotective effect, reducing neurodegeneration rates and improving behavior in mouse studies,[31] Figure 3.

Due to their numerous benefits, these compounds have garnered significant attention, prompting extensive research efforts over recent decades to synthesize derivatives containing the benzothiazole ring[32−34] and benzo[1,4]oxazin-3(4*H*)-one.[35−38] In pursuit of new compounds with diverse biological properties and practical applications, we have developed a series of straightforward, cost-effective procedures that yield high reaction efficiencies, enabling the synthesis of derivatives containing the benzothiazole bicyclic ring, as well as derivatives with both benzothiazole and benzoxazine-2-one bicyclic rings. To our knowledge, this study represents the first successful synthesis of a molecular scaffold containing both benzothiazole and benzo[1,4]oxazin-3(4*H*)-one bicyclic rings. Density functional theory (DFT) computational predictions were utilized to characterize the structures of the synthesized compounds.

■ RESULTS AND DISCUSSION

Amide **3** was synthesized from vanillin as previously reported by our research group.[39] However, the conversion of the nitro group to an amino group was successfully achieved using sodium dithionite,[40] resulting in a 92% yield, Scheme 1.

Amide **3** was reacted with ethyl chloroacetate in the presence of sodium iodide to produce ester **4**. Ester **4** was then hydrolyzed in a hot aqueous NaOH solution and immediately treated with dilute HCl to yield acid **5**. Subsequently, a coupling reaction was performed between acid **5** and amino acid esters, using the coupling reagent hexafluorophosphate azabenzotriazole tetramethyluronium (HATU) and *N*-methylmorpholine (NMM) as a base.[41] The crude reaction product was hydrolyzed with a NaOH solution and neutralized with dilute HCl without an intermediate purification step. This process yielded an unexpected product **U1** (R = H), in high yield, as confirmed by NMR spectral analysis. This unexpected outcome was replicated with various amino acids, resulting in additional unknown products **U2** (R = CH_3), **U3** (R = isopropyl), **U4** (R = *sec*-butyl), and **U5** (R = benzyl), Scheme 2.

Scheme 1. Synthesis of Compound Amide 3

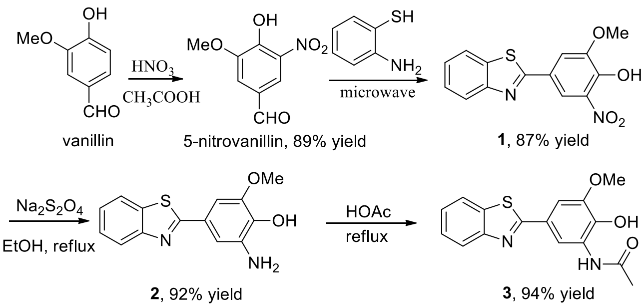

The mass spectra of unknown compounds **U1**, **U2**, **U3**, **U4**, and U**5** indicated a loss of two carbon units compared with the expected compounds, Figure S1 (Supporting Information). The ^{1}H NMR spectra displayed a new resonance corresponding to two protons (H28) with an unusually high chemical shift, exceeding 4.6 ppm. Specifically, the chemical shifts were as follows: compound **12a**, 4.67 ppm (s, 2H); **12b**, 4.69 ppm (d, *J* = 16.8 Hz, 1H) and 4.63 ppm (d, *J* = 16.8 Hz, 1H); **12c**, 4.82 ppm (d, *J* = 16.8 Hz, 1H) and 4.67 ppm (d, *J* = 16.2 Hz, 1H); **12e**, 4.81 ppm (d, *J* = 16.8 Hz, 1H) and 4.64 ppm (d, *J* = 16.8 Hz, 1H); **12f**, 4.52 ppm (d, *J* = 16.0 Hz, 1H) and 4.58 ppm (d, *J* = 15.0 Hz, 1H). Notably, the resonance corresponding to the H_3CCONH group was absent.

Heteronuclear multiple bond correlation (HMBC) spectra of compounds **12a** and **12b** showed that H28 interacts with C29, C16, and C15, as well as with the NH group. Unexpectedly, H28 also appears to interact with C10—an interaction not predicted in the expected compounds. In contrast, the nuclear Overhauser effect spectroscopy (NOESY) spectrum of compound **2** showed no significant correlation peaks, suggesting that H28 is far from H9. Based on these unusual spectral results, the research team proposed two possible structures for the unknown compounds, labeled as **I** and **II**, see Figure 4. However, it is expected that H15 and H28 in structure **I** would interact due to their presence within an oxazine ring, which is known to adopt certain conformations. Thus, structure **II** is more consistent with the spectral data presented.

To investigate the role of HATU in forming these unexpected products, we hypothesize that the absence of purification during the coupling of acid and amino acid ester with HATU may have led to an impure product, which was subsequently hydrolyzed in the next step. This suggests that the abnormal product formation could be attributed to the presence of HATU in the crude reaction mixture during hydrolysis. Based on this hypothesis, the research group introduced a purification step for the coupling reaction product using HATU before proceeding with hydrolysis. This approach yielded compounds **7a−f**, consistent with the initial predictions, partially validating the proposed role of HATU in the cyclization of the oxazine ring. The synthesis scheme of target compounds, incorporating the purification of intermediate products, is presented in Scheme 3.

Scheme 2. Formation of Compounds U1−U5 in the Presence of HATU from Compound 3

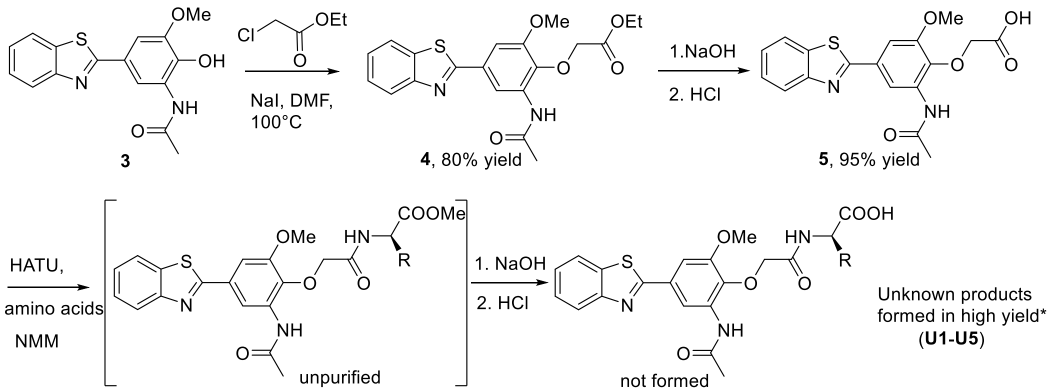

*The yields of the unknown products were determined after accurately identifying their structures by comparing the spectral data with the target product from the procedure presented in **Scheme 5**.
R = H: **12a** (**U1**), 92% yield
R = CH_3: **12b** (**U2**), 87% yield
R = Isopropyl: **12c** (**U3**), 89% yield
R = 2-methylpropan-1-yl: **12d**(**U4**), 87% yield
R = sec-butyl: **12e**, 93% yield
R = benzyl: **12f** (**U5**), 83% yield

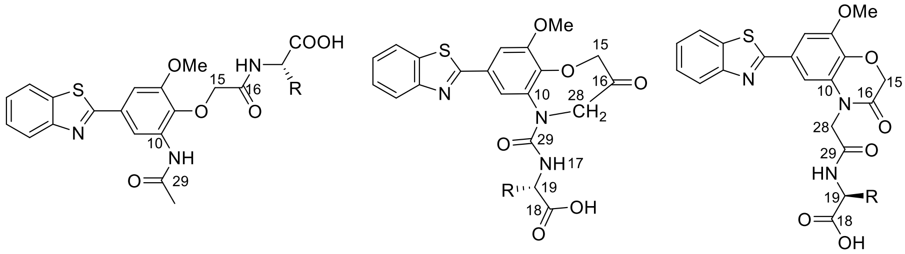

expected product   Structure **I**   Structure **II**

Figure 4. Structure of the expected product and the proposed structures **I** and **II** of the unknown product.

Scheme 3. Synthesis of Compounds 7a−f from Pure 6a−f

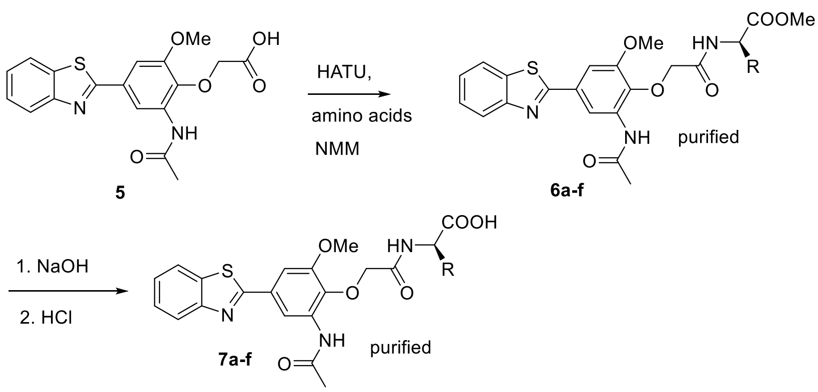

R= H (**6a**), 80% yield	R= H (**7a**), 92% yield
R = CH_3 (**6b**), 90% yield	R = CH_3 (**7b**), 93% yield
R = Isopropyl (**6c**), 82% yield	R = Isopropyl (**7c**), 90% yield
R = 2-methylpropan-1-yl (**6d**), 77% yield	R = 2-methylpropan-1-yl (**7d**), 95% yield
R = sec-butyl (**6e**), 72% yield	R = sec-butyl (**7e**), 96% yield
R = benzyl (**6f**), 86% yield	R = benzyl (**7f**), 93% yield

Due to the poor quality of crystals for the X-ray experiment, structure **II** was synthesized via an alternative route starting from known compound **2**. First, a retrosynthetic analysis of structure **II** was conducted, as shown in Scheme 4. Cleavage of the amide bond in structure **II** yields acid **10** and amino acids. Compound **10** can be synthesized from compound **8** and ethyl chloroacetate. Compound benzo[1,4]oxazin-3(4*H*)-one **8** was obtained from compound **2** and ethyl chloroacetate, Scheme 4.

Second, the unknown compounds with structure **II** were successfully synthesized. Treatment of compound **2** with ethyl chloroacetate yielded compound **8** in an 82% yield.[42] A subsequent reaction with an additional equivalent of ethyl chloroacetate in the presence of potassium carbonate produced

https://doi.org/10.1021/acsomega.4c06760
ACS Omega 2025, 10, 10835−10851

Scheme 4. Retrosynthesis of Structure II

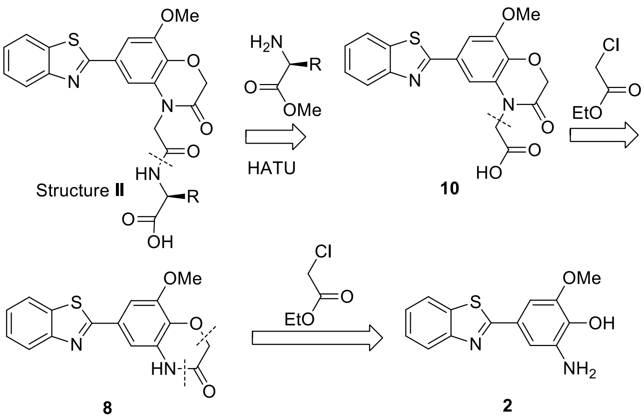

ester **9**.[43] Hydrolysis of ester **9** yielded carboxylic acid **10**, which was then coupled with various amino acid esters to produce compounds **11a–f**. These were subsequently hydrolyzed with sodium hydroxide in water–methanol solution and neutralized with dilute hydrochloric acid to obtain compounds **12a–f**, as shown in Scheme 5. Notably, the ^{1}H NMR spectra of compound **12a** fully aligned with structure **II**, Scheme 4.

Proposed Mechanism. An important question to address is how structure **II** was formed. Baumgarten et al. elucidated the existence of aziridin-2-one, showing that when nucleophilic substitution occurs on nitrogen bearing a good living group, aziridin-2-one can be opened by a nucleophile under basic conditions, breaking the (O═)C–N bond to form a secondary amine.[44] In our case, we propose the following mechanism for the formation of the benzo[1,4]oxazin-3(4*H*)-one structure **II** in the final stage, Schemes 6 and 7. The presence of HATU appears to facilitate the formation of an intermediate compound containing an α-lactam. In subsequent stages, a rearrangement occurs under basic conditions involving the three-membered intermediate compound described, proceeding through a two-step rearrangement. This ultimately leads to the formation of structure **II**, resulting in the fusion of benzothiazole and benzo[1,4]oxazin-3(4*H*)-one moieties via a Favorskii-like rearrangement.[45]

Additionally, DFT calculations with the B3LYP (Becke, 3-parameter, Lee–Yang–Parr) functional[46] at the 6-311++G-(d,p)[47] level have been employed to further elucidate the mechanism of α-lactam ring opening, leading to the formation of structure **II**. The B3LYP functional is widely recognized for its reliability in optimizing organic compound structures, providing accurate results.[48] Noncovalent interaction (NCI) analysis, also known as the reduced density gradient (RDG) method, serves as a powerful tool to examine noncovalent interaction within a molecule, such as van der Waals forces, hydrogen bonding, steric repulsion, and dispersion effects.[49] The molecular topological graph (green lines) obtained from atoms in molecules (AIM) calculations confirm the presence of N–H···O hydrogen bonds in the structures under investigation.[50] Figure 5 depicts the analysis conducted using NCI and AIM with the B3LYP/6-311++G(d,p) method. In the RGD isosurface, red zones correspond to repulsive interactions, indicated by the positive sign of $(\lambda 2)\rho(r)$. Green areas in the image signify regions where $\lambda 2$ values are near zero, indicating weak and delocalized interactions, typically found at the center of benzene rings and between various molecular groups. Conversely, blue regions with negative $\lambda 2$ values represent zones of attractive noncovalent interactions, such as hydrogen bonds, with stronger interactions indicated by darker shades of blue, particularly in N–H···O interactions.

We hypothesize that the transfer of hydrogen atoms from the nitrogen atom to the oxygen atom in the α-lactam moiety is a crucial step in the formation of structure **II**.

To further support the proposed reaction mechanism for the formation of structure **II**, we will use the representative compound **12b**. The optimized geometries of the reactants, intermediates, transition structures, and relative energies ΔE (kcal/mol) for the reaction involving **12b** are represented in Figure 6, with the energy level of the reactants (RA) set to zero. The symbols IS*x*, IS*y*, and IS*z* (IS1, IS2, etc.) and T*x*/*y* and T*y*/*z* (T1/2, T2/3, etc.) are used to denote the intermediate compounds and the transition states that link these intermediates. Vibrational frequencies were calculated at

Scheme 5. Synthesis of Compounds 12a–f from Compound 2

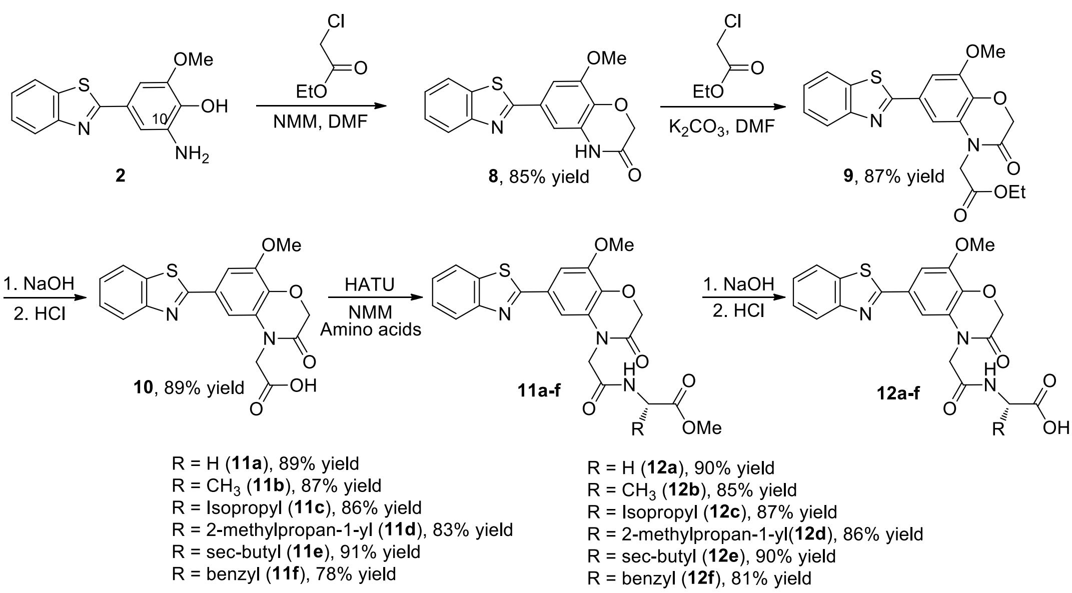

https://doi.org/10.1021/acsomega.4c06760
ACS Omega 2025, 10, 10835–10851

Scheme 6. Proposed Mechanism of Forming Compound α-Lactam

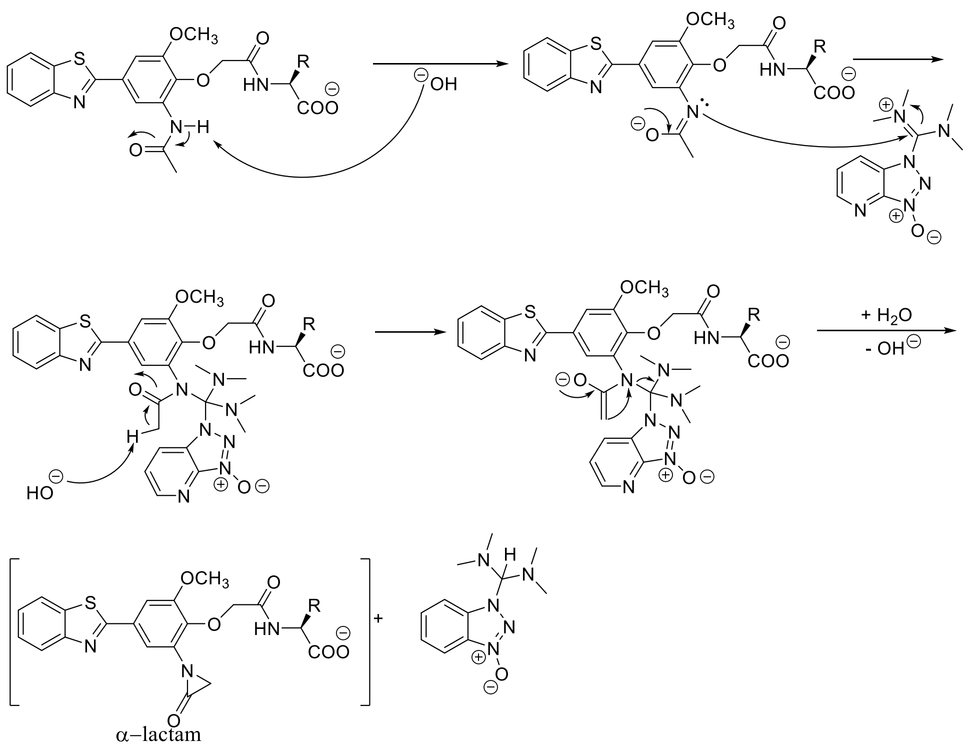

Scheme 7. α-Lactam Opening to Form Structure II

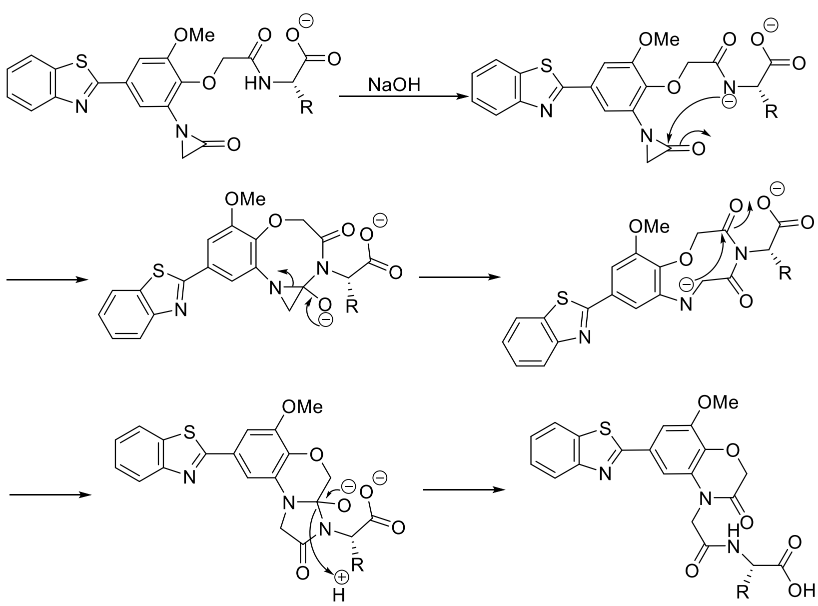

the same levels to confirm that the ground states showed no imaginary frequencies. A scheme illustrating the reaction pathways for compounds **12a**−**12f** is provided in Figure 7.

The reactions along the pathway display a thermodynamically downhill trend from IS2 to PR and from T1/2 to T3/4, indicating that these reactions are likely to occur spontaneously due to their overall exothermic nature (Figures 6 and 7). In the later stages, the previously mentioned three-membered intermediate undergoes rearrangement through a two-step process (Figure 8). Analyzing the entire pathway, we found that the T1/2 transition state represents the highest energy barrier, making it the rate-determining step of the overall processes (Table 1). However, this energy requirement is not a concern, as the preceding reactions are exothermic, allowing the T1/2 barrier to be surmountable.

The barrier energies of the pathways are very close (see Figure 7), indicating that they have nearly the same reactivity for the formation of structure **II**. In all ring-closure reactions, the rate-determining step is the transfer of a hydrogen atom from the nitrogen atom to the oxygen atom of the α-lactam moiety. As shown in Table 1, the reaction abilities follow a slightly decreasing order: **12d** > **12a** > **12f** > **12b** > **12c** > **12e**.

Furthermore, the notable difference in reactivity between **12d** and **12e** will be explained in the following analysis.

https://doi.org/10.1021/acsomega.4c06760
ACS Omega 2025, 10, 10835−10851

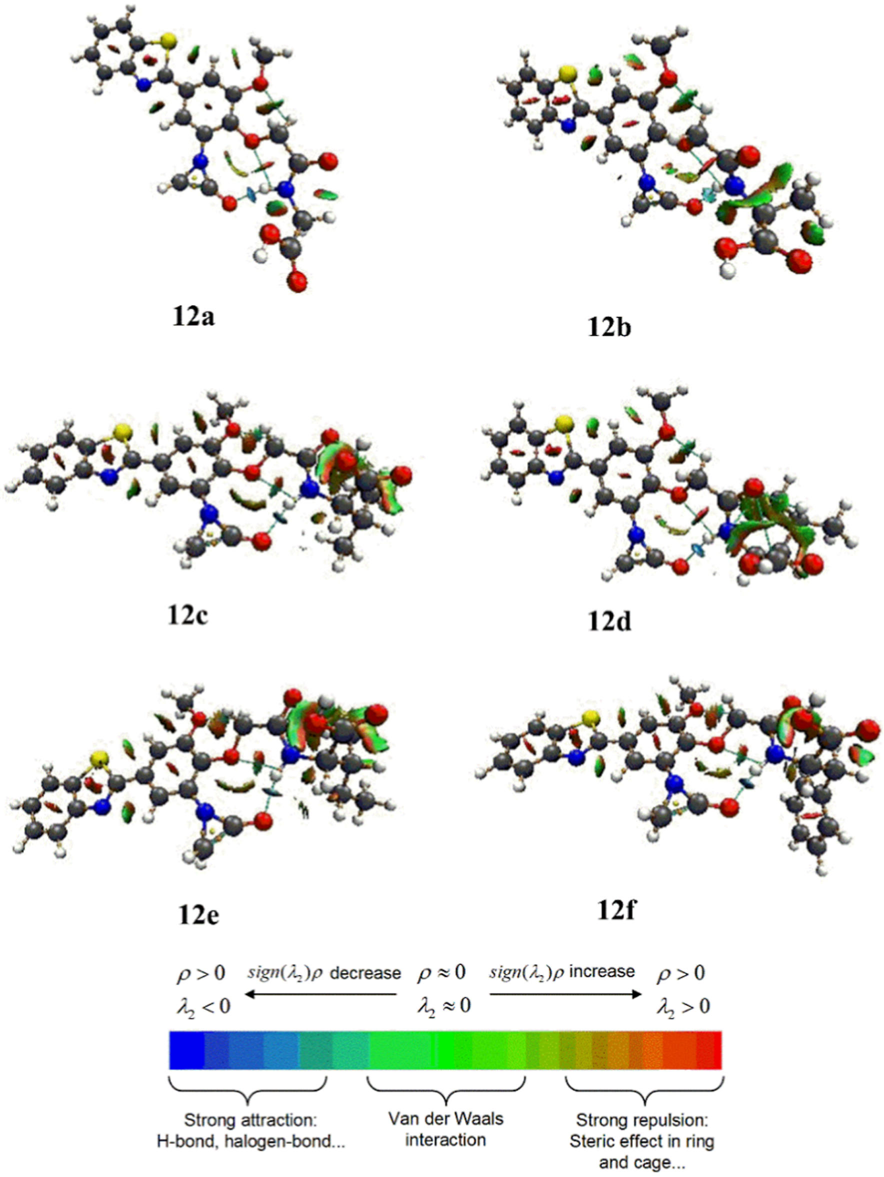

Figure 5. Isosurface map of RDG for **12a**−**12f** compounds. The isovalue of RDG is chosen to be 0.6. The molecular topological graph of the corresponding structures with the green lines are bond paths.

The +I (inductive) effect of the $-CH(CH_3)C_2H_5$ radical in **12e** is greater than that of the $-CH(CH_3)_2$ radical, which pushes electron density toward the nitrogen atom, increasing electron density on nitrogen. Consequently, the nitrogen−hydrogen interaction is stronger with the $-CH(CH_3)C_2H_5$ group in **12e** than that with the $-CH(CH_3)_2$ group in **12d**. As a result, hydrogen transfer in compound **12d** is more likely to occur than that in compound **12e**.

The hydrogen bond energy of the O···H−N bond was calculated using Espinosa's empirical formula, which relies on the electron density distribution at the bond critical points (BCPs) of the bond, expressed as $E_{HB} = 0.5\ V(r)$, where $V(r)$ represents the local energy density at the BCP.[51] A more negative E_{HB} value indicates greater bond stability. The results in Table 2 show that the tendency for the formation of the O−H bond decreases in the order: **12d** > **12a** > **12f** > **12b** > **12c** > **12e**.

We also account for this phenomenon by comparing the second-order stabilization energies of configurations **12d** and **12e**. Natural bond order (NBO) analysis of compounds **12d** and **12e** was conducted using second-order perturbation theory, where the second-order stabilization energy reflects the strength of the electron donor−acceptor interaction. Figure 9 illustrates the NBO overlap of electron donation from the lone pair of oxygen atoms to the antibonding acceptors of σ^*(N−H) in **12d** and **12e**. This donation from the lone pair of oxygen atoms to the antibonding orbital of the N−H bond facilitates breaking of the N−H bond and formation of a new O−H bond in the IS2. The second-order stabilization energy, presented in Figure 10, is 8.29 kcal/mol for the LP(O27) → σ^*(N18−H19) interaction in T1/2 (path from **12d**), which is greater than the LP(O27) → σ^*(N18−H44) interaction in T1/2 (path from **12e**, 7.79 kcal/mol). Consequently, the product derived from **12d** is more thermodynamically favored than that from **12e**.

In general, the energy barriers can be overcome by the energy released from the exothermic reaction, making the

https://doi.org/10.1021/acsomega.4c06760
ACS Omega 2025, 10, 10835−10851

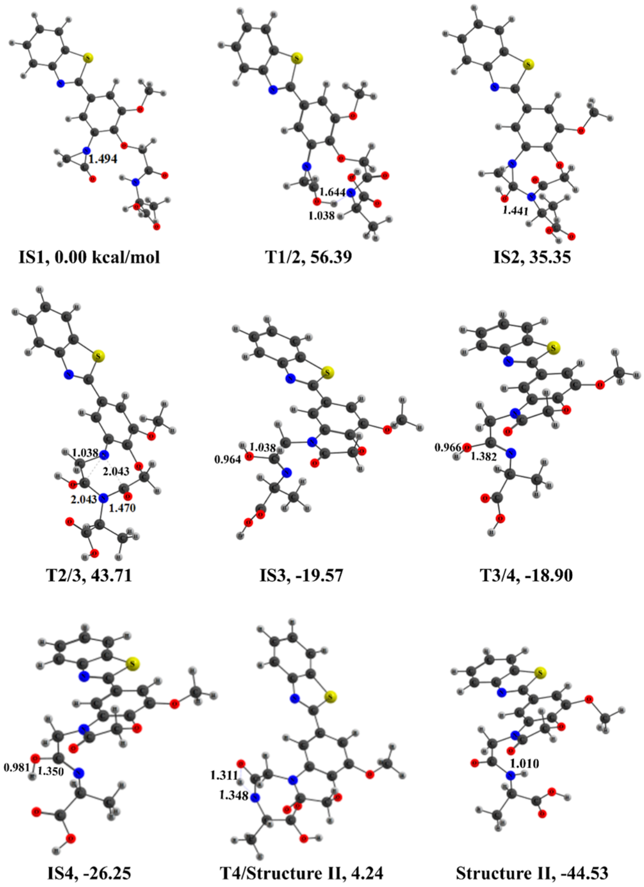

Figure 6. Optimized structures of the path form structure **II** from **12b** compound at the B3LYP/6-311++G(d,p) level.

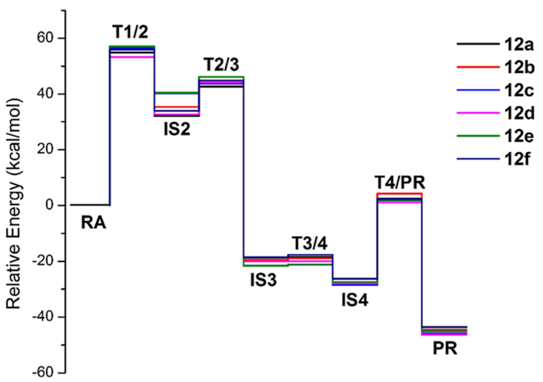

Figure 7. Profile of the potential energy surface for the formed structure II from **12a**−**12f** at the B3LYP/6-311++G(d,p) level.

overall reactions thermodynamically feasible for the formation of structure **II**.

Evaluation of the in vitro enzyme AChE inhibition activity of the synthesized derivatives:

Eighteen synthesized derivatives were selected for testing in vitro enzyme AChE inhibition activity, and the results are shown in Table 3.

Of the 18 compounds tested, only **6d** and **6f** demonstrated significant AChE inhibitory activity, with IC_{50} values of 32.00 and 25.33 μg/mL, respectively. Although these IC_{50} values differ from that of the standard compound donepezil, the results indicate the potential for these compounds in future AD treatment applications.

Molecular Docking and Molecular Dynamics. Based on the in vitro results, compounds **6d** and **6f**, which showed AChE inhibitory activity, were further analyzed to understand their interaction mechanisms and binding affinities within the AChE enzyme's active site. Calculations were performed using AutoDock Vina v1.2.3. Validation of the docking protocol was conducted by overlaying the cocrystallized ligand donepezil, as shown in Figure 10, yielding a computed Root Mean Square Deviation (RMSD) value of 0.234258 (<2 Å), which indicates accurate prediction of receptor−ligand complex conformations. Subsequently, compounds **6d** and **6f** were docked into the active site, resulting in binding energies of −8.463 and −9.613 kcal/mol, respectively, which aligns with in vitro results (IC_{50} of **6d** > IC_{50} of **6f**). Detailed interactions of the two compounds are illustrated in Figure 11. Compound **6d** forms hydrogen bonds with residues Tyr341, Phe295, and Tyr124, along with a pi−sulfur interaction with Tyr341 and pi−alkyl interactions with Trp286, Tyr337, and Trp86. Compound **6f**, meanwhile, establishes three hydrogen bonds with Tyr124, Tyr337, and Tyr341, as well as pi−pi and pi−alkyl interactions with Trp286 (Figure 11). Notably, these amino acid residues are located within the key catalytic sites PAS and CAS of the AChE enzyme, providing insight into the effective inhibition by these compounds.[52,53]

To monitor structural changes, we analyzed the differences in structural stability of the backbone atoms in three systems, 4EY7−**6d**, 4EY7−**6f**, and 4EY7−donepezil, using rmsd values.[54] The rmsd values of the test complexes were compared with those of the reference complex (4EY7−donepezil) and protein backbone atoms. Figure 12 illustrates the rmsd profiles of each system. Notably, the 4EY7−**6f** complex exhibited significantly greater stability than the 4EY7−**6d** complex after 200 ns of simulation, with an rmsd of 0.16361 nm compared to average rmsd values of 0.177 and 0.192 nm for the reference complex and protein backbone atoms, respectively. At the molecular level, compound **6f** forms a highly stable complex within the AChE active site, which enables selective inhibition of the protein's critical biological functions. Furthermore, the **6f**−AChE complex shows only slight fluctuations between 30 and 50 ns, stabilizing after 50 ns through the end of the simulation with an average rmsd of 0.162 nm. In comparison, the average rmsd values for **6d** and donepezil were 0.174 and 0.195 nm, respectively. Overall, the rmsd analysis suggests that the compounds identified in this study have promising potential as candidates for AD therapy.

■ EXPERIMENTAL SECTION

Chemistry. *General.* Solvents and other chemicals purchased from Sigma-Aldrich, Merck Corp., Aladdin, Vietnam, or other Chinese companies were used as received, unless indicated. NMR spectra were recorded on a Bruker AVANCE 600 MHz spectrometer in DMSO-d_6 at 298−300 K. Chemical-shift data for each signal was reported in ppm units. IR spectra were recorded on a Mattson 4020 GALAXY Series FT-IR. Mass spectra were recorded on an Agilent LC-MSD-Trap-SL series 1100 spectrometer. Melting points were measured by using a Gallenkamp melting point apparatus. A domestic oven Sharp R-205VN-S, made in China in 2022, was used to perform the reactions. In this study, the Gaussian 09 software package[55] was used to carry out standard electronic structure theory computations for all relevant compounds. The MultiWFN software package[50] was utilized for AIM analysis, and the isosurfaces were visualized using the VMD software

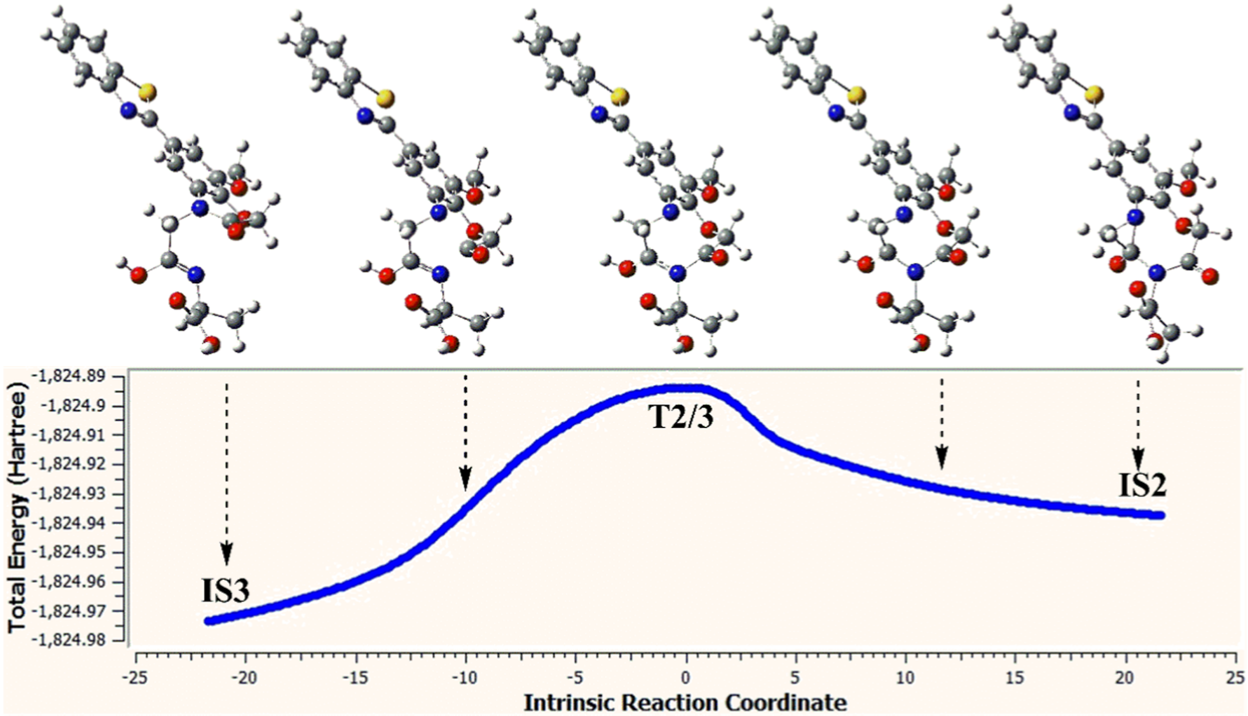

Figure 8. Visual representation of some specific IRC points along the pathway forming structure **II** from **12b**.

Table 1. Relative Energy (kcal/mol) of Species in Paths Forming Structure II From 12a−12f

	12a	12b	12c	12d	12e	12f
RA	0	0	0	0	0	0
T1/2	54.88	56.39	56.55	53.27	57.12	55.94
IS2	32.11	35.35	40.26	32.63	40.48	33.93
T2/3	42.65	43.71	43.84	44.14	46.16	44.90
IS3	−18.79	−19.57	−21.55	−20.02	−21.62	−18.51
T3/4	−18.43	−18.90	−21.16	−19.98	−21.25	−17.68
IS4	−26.19	−26.25	−28.52	−27.94	−27.43	−26.28
T4/PR	2.44	4.24	1.86	1.07	1.95	2.37
PR (structure **II**)	−43.57	−44.53	−45.81	−46.31	−45.02	−43.71

Table 2. Potential Energy Density [$V(r)$] and Hydrogen Energy E_{HB} for the O···H−N Bond in Complexes

complexes	$\rho(r)$ (au)	$V(r)$ (au)	E_{HB} (kcal/mol)
12a	0.027272	−0.023579	−7.40
12b	0.026587	−0.022972	−7.21
12c	0.026418	−0.022825	−7.16
12d	0.027331	−0.023618	−7.41
12e	0.021571	−0.018224	−5.72
12f	0.026682	−0.023021	−7.22

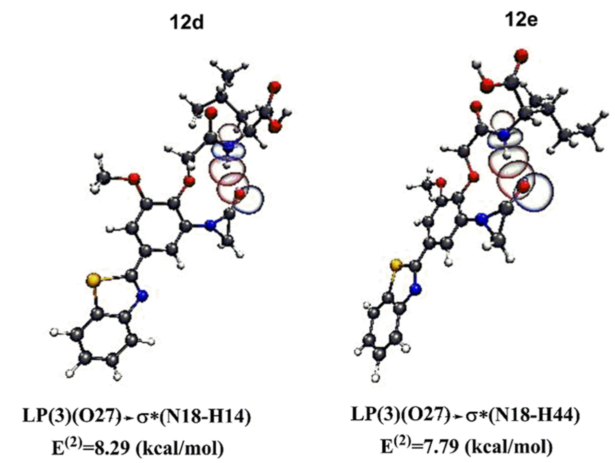

Figure 9. NBO analysis of donor−acceptor interaction for the **12d** and **12e** compounds is from calculations at the B3LYP/6-311++G(d,p) level. The values are the second-order stabilization energies.

package.[56] The AutoDock Vina 1.2.3[57] and GROMACS programs[58] were employed for molecular docking and molecular dynamics (MD) simulations, respectively.

Preparation. Procedure 1. A mixture of compound **5** (353 mg, 1 mmol), the methyl ester of amino acids (1 mmol), HATU (380 mg, 1 mmol), and NMM (330 mg, 3 mmol) was thoroughly mixed and added to a round-bottom flask containing 3 mL of *N*,*N*-dimethylformamide. The reaction mixture was stirred uniformly at 60 °C for 3 h. The progress of the reaction was monitored by thin-layer chromatography (TLC) (*n*-hexane/ethyl acetate, 2/1). Upon completion of the reaction, the solvent mixture was evaporated to yield a yellow-orange solid. Subsequently, the solid was recrystallized in ethanol/water (1:1, v/v) to afford compounds **6a-f** as white solids.

https://doi.org/10.1021/acsomega.4c06760
ACS Omega 2025, 10, 10835−10851

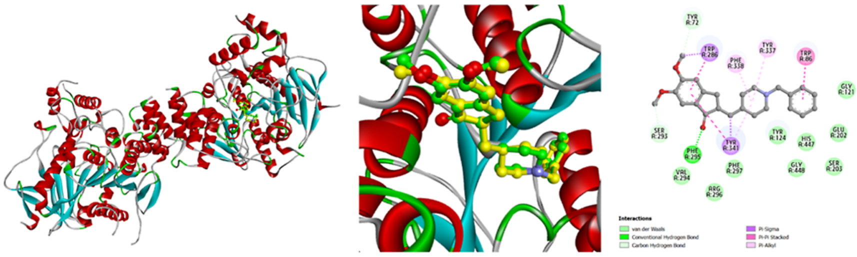

Figure 10. Redocking results of the cocrystallized ligand donepezil.

Table 3. Test Results of In Vitro Enzyme AChE Inhibitory Activity of Compounds 6a−6f, 7a−7f, and 12a−12f

no.	compound	AChE IC_{50} (μg/mL)	no.	compound	AChE IC_{50} (μg/mL)
1	**6a**	>128	11	**7e**	>128
2	**6b**	>128	12	**7f**	>128
3	**6c**	>128	13	**12a**	>128
4	**6d**	32.00 ± 2.07	14	**12b**	>128
5	**6e**	>128	15	**12c**	>128
6	**6f**	25.33 ± 1.98	16	**12d**	>128
7	**7a**	>128	17	**12e**	>128
8	**7b**	>128	18	**12f**	>128
9	**7c**	>128	19	donepezil	0.028 ± 0.003
10	**7d**	>128			

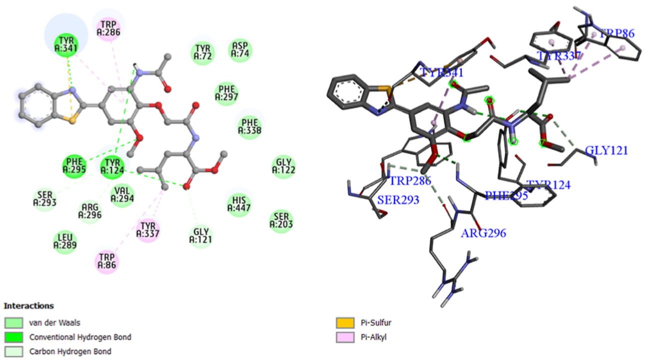

6d

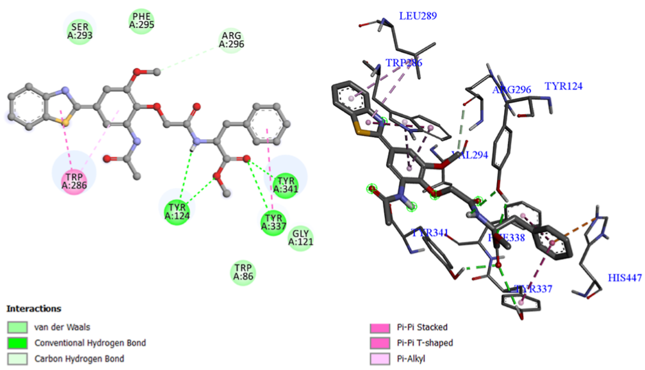

6f

Figure 11. 2D and 3D interactions of two compounds **6d** and **6f** within the active site of AChE (PDB ID: 4EY7).

Procedure 2. A mixture of compound **6** (5 mmol) was added to a round-bottom flask containing 5 mL of ethanol, followed by the addition of 10% NaOH solution (10 mL), and heated to reflux for approximately 5 min. The resulting reaction mixture was neutralized with 10% HCl or 10% H_2SO_4 solution until pH 4−5 was reached, forming a solid precipitate. Subsequently, the solid was filtered and washed with distilled water to obtain products **7a−f** as a white solids.

*Ethyl 2-(2-Acetamido-4-(benzothiazol-2-yl)-6-methoxyphenoxy)acetate (**4**).* A mixture of compound **3** (314 mg, 1 mmol), ethyl chloroacetate (1 mmol), K_2CO_3 (276 mg, 2 mmol), and NaI (150 mg, 1 mmol) was added to a round-bottom flask containing 10 mL of *N*,*N*-dimethylformamide and refluxed for 4 h. The progress of the reaction was monitored by TLC (*n*-hexane: ethyl acetate, 1/1(v/v)). Cold water was added to the crude mixture after a complete reaction to induce solid separation. The resulting solid was then filtered and washed with ethanol to afford the product **4** as a white solid (320 mg, 80%): mp 162−163 °C. HRMS (ESI-TOF) *m*/*z*: $[M + H]^+$ calcd for $C_{20}H_{21}N_2O_5S$, 401.11657; found, 401.11746. ^{1}H NMR (DMSO-d_6, 500 MHz): δ (ppm) 9.52 (s, 1H), 8.70 (d, J = 1.5 Hz, 1H), 8.03 (d, J = 2.0 Hz, 1H), 7.88 (d, J = 2 Hz, 1H), 7.57 (d, J = 1.5 Hz, 1H), 7.46 (dd, $J_1 = J_2$ = 7.5 Hz, 1H), 7.36 (dd, $J_1 = J_2$ = 7.5 Hz, 1H), 7.26 (s, 1H), 4.72 (s, 2H), 4.25 (q, 2H), 3.99 (s, 3H), 2.29 (s, 3H), and 1.30 (t, J = 7.5 Hz, 3H). ^{13}C NMR (DMSO-d_6, 125 MHz): δ (ppm) 171.6, 169.0, 167.9, 154.0, 151.7, 138.8, 135.4, 133.1, 130.0, 126.2, 125.0, 123.0, 121.6, 113.0, 105.3, 70.5, 61.8, 56.1, 24.7, and 14.1. ESI-MS, $[M + H]^+$, *m*/*z* (au)/relative intensity (%): 400.9/100.

*2-(2-Acetamido-4-(benzothiazol-2-yl)-6-methoxyphenoxy)acetic Acid (**5**).* A mixture of compound **4** (2 g, 5 mmol) was added to a round-bottom flask containing 5 mL of ethanol, followed by the addition of 10% NaOH solution (10 mL), and heated to reflux for approximately 5 min. The resulting reaction mixture was neutralized with 10% HCl or 10% H_2SO_4 solution until pH 4−5 was reached, forming a solid precipitate. Subsequently, the solid was filtered and washed with distilled water to obtain product **5** as a white solid (1.53 g, 95%). mp 231−232 °C. HRMS (ESI-TOF) *m*/*z*: $[M + H]^+$ calcd for $C_{18}H_{17}N_2O_5S$, 373.08527; found, 373.08633. ^{1}H NMR (DMSO-d_6, 500 MHz): δ (ppm) 9.88 (s, 1H), 8.60 (d, J = 1.5 Hz, 1H), 8.14 (d, J = 7.5 Hz, 1H), 8.07 (d, J = 7.5 Hz, 1H), 7.55 (ddd, J = 1.5 Hz, 7.0 Hz, 8.5 Hz, 1H), 7.49 (d, J = 1.5, 1H), 7.47 (td, J_1 = 1.5 Hz, $J_2 = J_3$ = 7.0 Hz, 1H), 4.71 (s, 2H), 3.96 (s, 3H), and 2.18 (s, 3H). ^{13}C NMR (DMSO-d_6, 125 MHz): δ (ppm) 172.6, 168.5, 166.9, 153.5, 151.9, 139.0, 134.4, 133.0, 128.6, 126.6, 125.4, 122.7, 122.2, 111.7, 105.5, 79.1, 69.7, 56.1, and 24.1. ESI-MS, $[M + H]^+$, *m*/*z* (au)/relative intensity (%): 372.9/100.

*Methyl (2-(2-Acetamido-4-(benzothiazol-2-yl)-6-methoxyphenoxy)acetyl)glycinate (**6a**).* Following procedure 1: a mixture of compound **5** (353 mg, 1 mmol), methyl ester of glycine (89 mg, 1 mmol), HATU (380 mg, 1 mmol), NMM (330 mg, 3 mmol), and *N*,*N*-dimethylformamide (3 mL) was stirred uniformly at 60 °C for 3 h. Recrystallization in ethanol: water (1:1, v/v) gave the product as a white solid (336 mg,

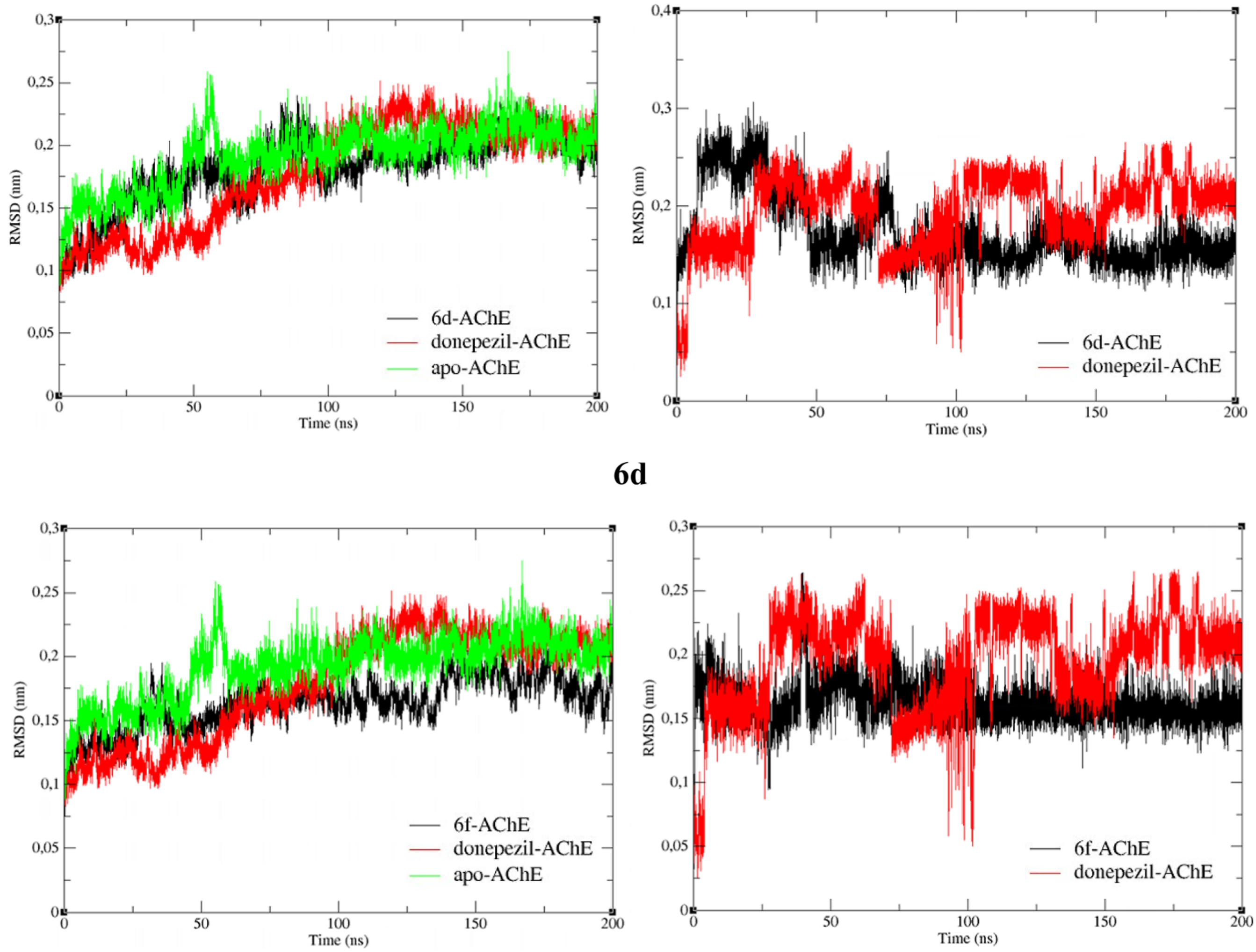

6f

Figure 12. Rmsd graph of the protein backbone (on the left) and the ligand in the complex (on the right).

80%): mp 220−222 °C. HRMS (ESI-TOF) m/z:[M + H]$^+$ calcd for $C_{21}H_{22}N_3O_6S$, 444.1224; found, 444.1205. ^{1}H NMR (DMSO-d_6, 600 MHz): δ (ppm) 10.10 (s, 1H), 8.73 (t, J = 6 Hz, 1H), 8.54 (d, J = 1.2 Hz, 1H), 8.14 (d, J = 7.8 Hz, 1H), 8.07 (d, J = 8.4 Hz, 1H), 7.56 (ddd, J_1 = 1.2 Hz, J_2 = J_3 = 8.4 Hz, 1H), 7.49 (d, J = 1.8, 1H), 7.46 (ddd, J_1 = 1.2 Hz, J_2 = J_3 = 8.4 Hz, 1H), 4.63 (s, 2H), 3.99 (d, J = 6 Hz, 2H), 3.72 (s, 3H), 3.66 (s, 3H), and 2.16 (s, 3H). ^{13}C NMR (DMSO-d_6, 150 MHz): δ (ppm) 170.0, 169.8, 168.6, 166.9, 153.5, 152.2, 139.4, 134.4, 133.0, 128.7, 126.6, 125.4, 122.7, 122.2, 112.3, 105.5, 71.4, 56.1, 51.7, 40.4, and 24.1. ESI-MS, [M + H]$^+$, m/z (au)/relative intensity (%): 443.9/100. [M − H]$^-$, m/z (au)/relative intensity (%): 441.9/100.

*Methyl (2-(2-Acetamido-4-(benzothiazol-2-yl)-6-methoxyphenoxy)acetyl)-L-alaninate (**6b**).* Following procedure 1: a mixture of compound **5** (353 mg, 1 mmol), methyl ester of alanine (103 mg, 1 mmol), HATU (380 mg, 1 mmol), NMM (330 mg, 3 mmol), and *N*,*N*-dimethylformamide (3 mL) was stirred uniformly at 60 °C for 3 h. Recrystallization in ethanol: water (1:1, v/v) gave the product as a white solid (390 mg, yield 90%): mp 227−229 °C. HRMS (ESI-TOF) m/z: [M + H]$^+$ calcd for $C_{22}H_{24}N_3O_6S$, 458.1380; found, 458.1360. ^{1}H NMR (DMSO-d_6, 600 MHz): δ (ppm) 10.19 (s, 1H), 8.69 (d, J = 7.2 Hz, 1H), 8.55 (d, J = 1.8 Hz, 1H), 8.13 (d, J = 7.8 Hz, 1H), 8.06 (d, J = 8.4 Hz, 1H), 7.54 (ddd, J_1 = J_2 = 7.2, J_3 = 1.2 Hz, 1H), 7.49 (d, J = 1.8 Hz, 1H), 7.46 (ddd, J_1 = J_2 = 7.2, J_3 = 1.2 Hz, 1H), 4.62 (q, J = 9.6 Hz, 2H), 4.43 (t, J = 7.2 Hz, 2H), 3.97 (s, 3H), 3.65 (s, 3H), and 2.16 (s, 3H). ^{13}C NMR (DMSO-d_6, 150 MHz): δ (ppm) 172.5, 169.5, 168.6, 166.9, 153.5, 152.2, 139.4, 134.4, 133.0, 128.8, 126.6, 125.4, 122.7, 122.3, 112.1, 105.5, 71.4, 56.1, 52.0, 47.4, 24.1, and 16.9. ESI-MS, [M + H]$^+$, m/z (au)/relative intensity (%): 459.0/100.

*Methyl (2-(2-Acetamido-4-(benzothiazol-2-yl)-6-methoxyphenoxy)acetyl)-L-valinate (**6c**).* Following procedure 1: a mixture of compound **5** (353 mg, 1 mmol), methyl ester of valine (131 mg, 1 mmol), HATU (380 mg, 1 mmol), NMM (330 mg, 3 mmol), and *N*,*N*-dimethylformamide (3 mL) was stirred uniformly at 60 °C for 3 h. Recrystallization in ethanol: water (1:1, v/v) gave the product as a white solid (355 mg, yield 82%): mp 232−233 °C. HRMS (ESI-TOF) m/z: [M + H]$^+$ calcd for $C_{24}H_{28}N_3O_6S$, 486.1693; found, 486.1691. ^{1}H NMR (DMSO-d_6, 600 MHz): δ (ppm) 10.30 (s, 1H), 8.71 (d, J = 8.4 Hz, 1H), 8.12 (d, J = 7.8 Hz, 1H), 8.01 (d, J = 8.4 Hz, 1H), 7.54 (dd, J_1 = J_2 = 7.8 Hz, 1H), 7.49 (d, J = 1.8 Hz, 1H), 7.44−7.47 (m, 1H), 7.43 (d, J = 1.8 Hz, 1H), 7.22 (d, J = 1.2 Hz, 1H), 4.78 (s, 3H), 4.68−4.70 (m, 2H), 3.94 (s, 3H), 3.60 (s, 3H), 2.07−2.16 (m, 1H), and 0.88−0.93

https://doi.org/10.1021/acsomega.4c06760
ACS Omega 2025, 10, 10835−10851

(m, 6H). ^{13}C NMR (DMSO-d_6, 150 MHz): δ (ppm) 171.6, 171.4, 168.5, 166.5, 153.3, 152.2, 136.5, 134.4, 130.1, 126.9, 125.3, 122.5, 122.1, 112.1, 106.5, 66.8, 57.4, 56.2, 51.7, 30.0, 29.9, 18.9, and 18.0. ESI-MS, $[M + H]^+$, m/z (au)/relative intensity (%): 486.9/100. $[M - H]^-$, m/z (au)/relative intensity (%): 483.8/100.

*Methyl (2-(2-Acetamido-4-(benzothiazol-2-yl)-6-methoxyphenoxy)acetyl)-L-leucinate (**6d**).* Following procedure 1: a mixture of compound **5** (353 mg, 1 mmol), methyl ester of leucine (145 mg, 1 mmol), HATU (380 mg, 1 mmol), NMM (330 mg, 3 mmol), and *N,N*-dimethylformamide (3 mL) was stirred uniformly at 60 °C for 3 h. Recrystallization in ethanol: water (1:1, v/v) gave the product as a white solid (364 mg, yield 77%): mp 237−239 °C. HRMS (ESI-TOF) m/z: $[M + H]^+$ calcd for $C_{25}H_{30}N_3O_6S$, 500.1850; found, 500.1850. ^{1}H NMR (DMSO-d_6, 600 MHz): δ (ppm) 10.19 (s, 1H), 8.67 (d, J = 7.8 Hz, 1H), 8.56 (d, J = 1.8 Hz, 1H), 8.14 (d, J = 7.2 Hz, 1H), 8.07 (d, J = 7.8 Hz, 1H), 7.55 (ddd, J_1 = 1.2 Hz, J_2 = J_3 = 7.8 Hz, 1H), 7.49 (d, J = 2.4 Hz, 1H), 7.46 (ddd, J_1 = 1.2 Hz, J_2 = J_3 = 7.8 Hz, 1H), 4.65 (q, J = 15.6 Hz, 2H), 4.43−4.45 (m, 1H), 3.97 (s, 3H), 3.65 (s, 3H), 2.16 (s, 3H), 1.54−1.64 (m, 2H), 1.55 (dd, J = 5.4, 10.2 Hz, 1H), 0.89 (d, J = 6.6 Hz, 1H), and 0.86 (d, J = 6.0 Hz, 1H). ^{13}C NMR (DMSO-d_6, 150 MHz): δ (ppm) 172.4, 169.8, 168.6, 166.9, 153.5, 152.2, 139.3, 134.4, 133.0, 128.8, 126.6, 125.4, 122.7, 122.7, 122.3, 112.1, 105.4, 71.4, 56.0, 51.9, 50.1, 24.1, 22.6, and 21.1. ESI-MS, $[M + H]^+$, m/z (au)/relative intensity (%): 50.1/100.

*Methyl (2-(2-Acetamido-4-(benzothiazol-2-yl)-6-methoxyphenoxy)acetyl)-L-alloisoleucinate (**6e**).* Following procedure 1: a mixture of compound **5** (353 mg, 1 mmol), methyl ester of isoleucine (145 mg, 1 mmol), HATU (380 mg, 1 mmol), NMM (330 mg, 3 mmol), and *N,N*-dimethylformamide (3 mL) was stirred uniformly at 60 °C for 3 h. Recrystallization in ethanol: water (1:1, v/v) gave the product as a white solid (341 mg, yield 72%): mp 238−240 °C. HRMS (ESI-TOF) m/z: $[M + H]^+$ calcd for $C_{25}H_{30}N_3O_6S$, 500.1850; found, 500.1836. ^{1}H NMR (DMSO-d_6, 600 MHz): δ (ppm) 10.29 (s, 1H), 8.56 (d, J = 1.8 Hz, 1H), 8.55 (d, J = 7.8 Hz, 1H), 8.13 (d, J = 7.8 Hz, 1H), 8.07 (d, J = 7.8 Hz, 1H), 7.55 (td, J_1 = 1.2 Hz, J_2 = J_3 = 8.4 Hz, 1H), 7.48 (d, J = 1.8 Hz, 1H), 7.46 (ddd, J_1 = 1.2 Hz, J_2 = J_3 = 8.4 Hz, 1H), 4.68 (q, J = 15 Hz, 2H), 4.35 (q, J = 6.6 Hz, 1H), 3.97 (s, 3H), 3.65 (s, 3H), 2.16 (s, 3H), 1.78−1.85 (m, 1H), 1.38−1.41 (m, 1H), 1.17−1.21 (m, 1H), and 0.83−0.86 (m, 6H). ^{13}C NMR (DMSO-d_6, 150 MHz): δ (ppm) 171.5, 170.1, 168.6, 167.0, 153.5, 152.2, 139.4, 134.5, 133.2, 128.8, 126.6, 125.4, 122.7, 122.3, 112.0, 105.4, 71.5, 56.3, 56.1, 51.7, 24.6, 24.1, 15.3, and 11.0. ESI-MS, $[M + H]^+$, m/z (au)/relative intensity (%): 500.0/100. $[M - H]^-$, m/z (au)/relative intensity (%): 498.0/100. $[\alpha]_D^{20}$ −33.6 (c 0.11, $CHCl_3$).

*Methyl (2-(2-Acetamido-4-(benzothiazol-2-yl)-6-methoxyphenoxy)acetyl)-L-phenylalaninate (**6f**).* Following procedure 1: a mixture of compound **5** (353 mg, 1 mmol), methyl ester of phenylalanine (179 mg, 1 mmol), HATU (380 mg, 1 mmol), NMM (330 mg, 3 mmol), and *N,N*-dimethylformamide (3 mL) was stirred uniformly at 60 °C for 3 h. Recrystallization in ethanol: water (1:1, v/v) gave the product as a white solid (434 mg, yield 86%): mp 230−232 °C. HRMS (ESI-TOF) m/z: $[M + H]^+$ calcd for $C_{28}H_{28}N_3O_6S$, 534.1693; found, 500.1670. ^{1}H NMR (DMSO-d_6, 600 MHz): δ (ppm) 10.10 (s, 1H), 8.72 (d, J = 7.8 Hz, 1H), 8.54 (s, 1H), 8.13 (d, J = 7.8 Hz, 1H), 8.07 (d, J = 7.8 Hz, 1H), 7.54 (dd, J_1 = J_2 = 8.4 Hz, 1H), 7.47 (d, J = 1.8 Hz, 1H), 7.46 (dd, J_1 = J_2 = 7.8 Hz, 1H), 7.17−7.20 (m, 5H), 4.54−4.66 (m, 1H), 4.56 (q, J = 15 Hz, 2H), 3.93 (s, 3H), 3.62 (s, 3H), 3.10 (q, J = 8.4, 5.4 Hz, 1H), 2.94 (q, J = 9, 4.8 Hz, 1H), and 2.12 (s, 1H). ^{13}C NMR (DMSO-d_6, 150 MHz): δ (ppm) 171.3, 169.7, 168.5, 166.9, 153.5, 152.1, 139.2, 136.7, 134.4, 133.0, 128.9, 128.8, 128.1, 126.6, 126.5, 126.4, 122.7, 122.2, 112.1, 105.4, 71.3, 56.0, 53.3, 51.9, 36.6, and 24.11. ESI-MS, $[M + H]^+$, m/z (au)/relative intensity (%): 278.0/100. $[M - H]^-$, m/z (au)/relative intensity (%): 532.0/100.

*(2-(2-Acetamido-4-(benzothiazol-2-yl)-6-methoxyphenoxy)acetyl)glycine (**7a**).* Following procedure 2: a mixture of compound **6a** (2.22 g, 5 mmol), ethanol (5 mL), and 10% NaOH solution (10 mL) was heated to reflux for approximately 5 min. Recrystallization in ethanol/water (1:1, v/v) gave the product as a white solid (1.97 g, yield 92%): mp 258−260 °C. HRMS (ESI-TOF) m/z: $[M + H]^+$ calcd for $C_{20}H_{20}N_3O_6S$, 430.1067; found, 430.1079. ^{1}H NMR (DMSO-d_6, 600 MHz): δ (ppm) 10.18 (s, 1H), 8.62 (t, J = 5.4 Hz, 1H), 8,54 (d, J = 1.2 Hz, 1H), 8.14 (d, J = 8.4 Hz, 1H), 8.07 (d, J = 7.8 Hz, 1H), 7.54 (ddd, J_1 = 1.2 Hz, J_2 = J_3 = 8.4 Hz, 1H), 7.49 (d, J = 1.2 Hz, 1H), 7.46 (ddd, J_1 = 1.2 Hz, J_2 = J_3 = 7.2 Hz, 1H), 4.62 (s, 2H), 3.79 (s, 3H), 3.90 (d, J = 6 Hz, 2H), and 2.16 (s, 3H). ^{13}C NMR (DMSO-d_6, 150 MHz): δ (ppm) 170.7, 169.9, 168.6, 166.9, 153.5, 152.2, 139.4, 134.4, 133.0, 128.7, 126.6, 125.4, 122.7, 122.2, 112.3, 105.5, 71.5, 56.1, 40.4, and 24.1. ESI-MS, $[M + H]^+$, m/z (au)/relative intensity (%): 430.0/100. $[M - H]^-$, m/z (au)/relative intensity (%): 427.8/100.

*(2-(2-Acetamido-4-(benzothiazol-2-yl)-6-methoxyphenoxy)acetyl)-L-alanine (**7b**).* Following procedure 2: a mixture of compound **6b** (2.29 g, 5 mmol), ethanol (5 mL), and 10% NaOH solution (10 mL) was heated to reflux for approximately 5 min. Recrystallization in ethanol: water (1:1, v/v) gave the product as a white solid (2.2 g, yield 93%): mp 268−269 °C. HRMS (ESI-TOF) m/z: $[M + H]^+$ calcd for $C_{21}H_{22}N_3O_6S$, 444.1224; found, 444.1210. ^{1}H NMR (DMSO-d_6, 600 MHz): δ (ppm) 10.28 (s, 1H), 8.58 (d, J = 7.2 Hz, 1H), 8.50 (d, J = 1.8 Hz, 1H), 8.13 (d, J = 7.8 Hz, 1H), 8.07 (d, J = 7.8 Hz, 1H), 7.55 (ddd, J_1 = 1.2 Hz, J_2 = J_3 = 7.2 Hz, 1H), 7.49 (d, J = 2.4 Hz, 1H), 7.47 (ddd, J_1 = 1.2 Hz, J_2 = J_3 = 7.2 Hz, 1H), 4.63 (q, J = 15.6 Hz, 2H), 4.35 (t, J = 7.2 Hz, 1H), 3.97 (s, 3H), 2.16 (s, 3H), and 1.33 (d, J = 7.2 Hz, 3H). ^{13}C NMR (DMSO-d_6, 150 MHz): δ (ppm) 173.5, 169.4, 168.6, 166.9, 153.5, 152.2, 139.5, 134.4, 133.0, 128.7, 126.6, 125.4, 122.7, 122.2, 112.2, 105.5, 71.5, 56.0, 47.4, 24.1, and 17.1. ESI-MS, $[M + H]^+$, m/z (au)/relative intensity (%): 444.0/100. $[M - H]^-$, m/z (au)/relative intensity (%): 441.9/100.

*(2-(2-Acetamido-4-(benzothiazol-2-yl)-6-methoxyphenoxy)acetyl)-L-valine (**7c**).* Following procedure 2: a mixture of compound **6c** (2.43 g, 5 mmol), ethanol (5 mL), and 10% NaOH solution (10 mL) was heated to reflux for approximately 5 min. Recrystallization in ethanol/water (1:1, v/v) gave the product as a white solid (2.25 g, yield 90%): mp 277−279 °C. HRMS (ESI-TOF) m/z: $[M + H]^+$ calcd for $C_{23}H_{26}N_3O_6S$, 472.1537; found, 472.1524. ^{1}H NMR (DMSO-d_6, 600 MHz): δ (ppm) 8.56 (d, J = 1.8 Hz, 1H), 8.39 (d, J = 8.4 Hz, 1H), 8.13 (d, J = 7.2 Hz, 1H), 8.57 (d, J = 7.8 Hz, 1H), 7.54 (ddd, J_1 = 1.2 Hz, J_2 = J_3 = 8.4 Hz, 1H), 7.49 (d, J = 1.8 Hz, 1H), 7.46 (ddd, J_1 = 1.2 Hz, J_2 = J_3 = 8.4 Hz, 1H), 4.70 (q, J = 15.6 Hz, 2H), 4.27 (q, J = 6 Hz, 1H), 3.97 (s, 3H), 2.16 (s, 3H), 2.08−2.17 (m, 1H), and 0.9 (q, J = 5.4, 6H). ^{13}C

https://doi.org/10.1021/acsomega.4c06760
ACS Omega 2025, 10, 10835−10851

NMR (DMSO-d_6, 150 MHz): δ (ppm) 172.4, 170.1, 168.5, 167.0, 153.5, 152.2, 139.5, 134.4, 133.2, 128.8, 126.6, 125.4, 122.7, 122.2, 112.0, 105.4, 71.6, 57.2, 56.1, 29.8, 24.1, 18.9, and 17.8. ESI-MS, $[M + H]^+$, m/z (au)/relative intensity (%): 472.0/100. $[M - H]^-$, m/z (au)/relative intensity (%): 469.8/100.

*(2-(2-Acetamido-4-(benzothiazol-2-yl)-6-methoxyphenoxy)acetyl)-L-leucine (**7d**).* Following procedure 2: a mixture of compound **6d** (2.50 g, 5 mmol), ethanol (5 mL), and 10% NaOH solution (10 mL) was heated to reflux for approximately 5 min. Recrystallization in ethanol: water (1:1, v/v) gave the product as a white solid (2.44 g, yield 95%): mp 285−286 °C. HRMS (ESI-TOF) m/z: $[M + H]^+$ calcd for $C_{24}H_{28}N_3O_6S$, 486.1693; found, 486.1690. ^1H NMR (DMSO-d_6, 600 MHz): δ (ppm) 12.66 (s, 1H), 10.26 (s, 1H), 8.56 (d, J = 1.2 Hz, 1H), 8.53 (d, J = 7.8 Hz, 1H), 8.14 (d, J = 7.8 Hz, 1H), 8.07 (d, J = 7.8 Hz, 1H), 7.55 (ddd, J_1 = 1.2 Hz, $J_2 = J_3$ = 8.4 Hz, 1H), 7.49 (d, J = 1.8 Hz, 1H), 7.46 (ddd, J_1 = 1.2 Hz, $J_2 = J_3$ = 8.4 Hz, 1H), 4.65 (q, J = 9 Hz, 2H), 3.97 (s, 3H), 2.16 (s, 3H), 1.56−1.59 (m, 3H), and 0.88 (q, J = 6.6 Hz, 6H). ^{13}C NMR (DMSO-d_6, 150 MHz): δ (ppm) 173.4, 169.6, 168.5, 166.9, 153.5, 152.2, 139.4, 134.4, 133.0, 128.7, 126.6, 125.4, 122.7, 122.2, 112.1, 105.4, 71.5, 56.0, 50.1, 24.2, 24.1, 22.7, and 21.2. ESI-MS, $[M + H]^+$, m/z (au)/relative intensity (%): 486.0/100. $[M - H]^-$, m/z (au)/relative intensity (%): 483.9/100.

*(2-(2-Acetamido-4-(benzothiazol-2-yl)-6-methoxyphenoxy)acetyl)-D-alloisoleucine (**7e**).* Following procedure 2: a mixture of compound **6e** (2.50 g, 5 mmol), ethanol (5 mL), and 10% NaOH solution (10 mL) was heated to reflux for approximately 5 min. Recrystallization in ethanol/water (1:1, v/v) gave the product as a white solid (2.47 g, yield 96%): mp 287−289 °C. HRMS (ESI-TOF) m/z: $[M + H]^+$ calcd for $C_{24}H_{28}N_3O_6S$, 486.1693; found, 486.1683. ^1H NMR (DMSO-d_6, 600 MHz): δ (ppm) 12.65 (s, 1H), 10.27 (s, 1H), 8.56 (d, J = 1.2 Hz, 1H), 8.53 (d, J = 7.8 Hz, 1H), 8.14 (d, J = 7.8 Hz, 1H), 8.07 (d, J = 7.8 Hz, 1H), 7.55 (ddd, J_1 = 1.2 Hz, $J_2 = J_3$ = 8.4 Hz, 1H), 7.49 (d, J = 1.8 Hz, 1H), 7.46 (ddd, J_1 = 1.2 Hz, $J_2 = J_3$ = 8.4 Hz, 1H), 4.63 (q, J = 15.0 Hz, 2H), 4.26−4.28 (m, 1H), 3.97 (s, 3H), 2.16 (s, 3H), 0.89 (d, J = 6.6 Hz, 3H), and 0.86 (d, J = 6.6 Hz, 3H). ^{13}C NMR (DMSO-d_6, 150 MHz): δ (ppm) 170.4, 169.9, 168.5, 167.0, 153.5, 152.2, 139.5, 134.4, 133.2, 128.8, 126.6, 125.4, 122.7, 122.2, 112.0, 105.4, 71.6, 56.2, 56.0, 36.3, 24.5, 24.1, 15.4, and 11.2. ESI-MS, $[M + H]^+$, m/z (au)/relative intensity (%): 485.9/100. $[M - H]^-$, m/z (au)/relative intensity (%): 483.7/100.

*(2-(2-Acetamido-4-(benzothiazol-2-yl)-6-methoxyphenoxy)acetyl)-D-phenylalanine (**7f**).* Following procedure 2: a mixture of compound **6f** (2.67 g, 5 mmol), ethanol (5 mL), and 10% NaOH solution (10 mL) was heated to reflux for approximately 5 min. Recrystallization in ethanol: water (1:1, v/v) gave the product as a white solid (2.41 g, yield 93%): mp 280−282 °C. HRMS (ESI-TOF) m/z: $[M + H]^+$ calcd for $C_{27}H_{26}N_3O_6S$, 520.1537; found, 520.1515. ^1H NMR (DMSO-d_6, 600 MHz): δ (ppm) 12.93 (s, 1H), 10.25 (s, 1H), 8.58 (d, J = 7.8 Hz, 1H), 8.54 (s, 1H), 8.14 (d, J = 7.8 Hz, 1H), 8.07 (d, J = 8.4 Hz, 1H), 7.55 (dd, $J_1 = J_2$ = 7.2 Hz, 1H), 7.46 (d, J = 7.2 Hz, 1H), 7.47 (s, 1H), 7.16−7.24 (m, 5H), 4.59 (s, 2H), 4.55 (t, J = 12.0 Hz, 1H), 3.93 (s, 3H), 3.12 (dd, J = 4.8, 13.8 Hz, 1H), 3.92 (dd, J = 9.0, 13.8 Hz, 1H), and 2.13 (s, 3H). ^{13}C NMR (DMSO-d_6, 150 MHz): δ (ppm) 172.2, 169.6, 168.5, 166.9, 153.4, 152.1, 139.3, 137.2, 134.4, 133.0, 128.9, 128.7, 128.0, 126.5, 126.3, 125.3, 122.7, 122.2, 112.1, 105.4, 71.4, 56.0, 53.3, 36.7, and 24.1. ESI-MS, $[M + H]^+$, m/z (au)/relative intensity (%): 519.5/100. $[M - H]^-$, m/z (au)/relative intensity (%): 516.7/100.

*2-(6-(Benzothiazol-2-yl)-8-methoxy-3-oxo-2,3-dihydro-4H-benzo[1,4]oxazin-4-yl)acetic Acid (**10**).* Following the procedure for the synthesis of compound **5**: a mixture of compound **9** (1.99 g, 5 mmol), ethanol (5 mL), and 10% NaOH solution (10 mL) was heated to reflux for approximately 5 min. Recrystallization in ethanol/water (1:1, v/v) gave the product as a white solid (1.7 g, yield 89%): mp 265−267 °C. HRMS (ESI-TOF) m/z: $[M + H]^+$ calcd for $C_{18}H_{15}N_2O_5S$, 371.0696; found, 371.0685. ^1H NMR (DMSO-d_6, 600 MHz): δ (ppm) 13.24 (s, 1H), 8.13 (d, J = 7.8 Hz, 1H), 8.06 (d, J = 8.4 Hz, 1H), 7.54 (dd, $J_1 = J_2$ = 7.2 Hz, 1H), 7.46 (dd, $J_1 = J_2$ = 6.6 Hz, 2H), 7.29 (s, 1H), 4.80 (s, 2H), 4.77 (s, 2H), and 3.95 (s, 3H). ^{13}C NMR (DMSO-d_6, 150 MHz): δ (ppm) 169.2, 166.6, 164.1, 153.3, 148.8, 136.5, 134.4, 129.9, 127.1, 126.6, 125.3, 122.6, 122.2, 106.6, 106.3, 66.8, 56.2, and 42.7. ESI-MS, $[M + H]^+$, m/z (au)/relative intensity (%): 370.9/100. $[M - H]^-$, m/z (au)/relative intensity (%): 368.9/100.

*(2-(6-(Benzothiazol-2-yl)-8-methoxy-3-oxo-2,3-dihydro-4H-benzo[1,4]oxazin-4-yl)acetyl)glycine (**12a**).* Following the procedure for the synthesis of compound **7a**: a mixture of compound **11a** (2.21 g, 5 mmol), ethanol (5 mL), and 10% NaOH solution (10 mL) was heated to reflux for approximately 5 min. Recrystallization in ethanol: water (1:1, v/v) gave the product as a white solid (1.92 g, 90%): mp 283−284 °C. IR (ν, cm^{-1}): 3291 (NH), 1691, 1651 (C═O), 1611, 1562, 1527 (C═C, C═N). HRMS (ESI-TOF) m/z: $[M + H]^+$ calcd for $C_{20}H_1N_3O_6S$, 428.0911; found, 428.0902. ^1H NMR (DMSO-d_6, 600 MHz): δ (ppm) 8.60 (t, J = 5.4 Hz, 1H), 8.12 (d, J = 7.8 Hz, 1H), 8.05 (d, J = 7.8 Hz, 1H), 7.54 (ddd, J_1 = 1.2 Hz, $J_2 = J_3$ = 7.8 Hz, 1H), 7.49 (d, J = 1.2 Hz, 1H), 7.44 (ddd, J_1 = 1.2 Hz, $J_2 = J_3$ = 7.8 Hz, 1H), 7.21 (d, J = 1.2 Hz, 1H), 4.79 (s, 2H), 4.67 (s, 2H), 3.94 (s, 3H), and 3.80 (d, J = 5.4 Hz, 2H). ^{13}C NMR (DMSO-d_6, 150 MHz) δ (ppm):170.8, 166.8, 166.7, 163.9, 153.4, 148.7, 136.5, 134.5, 130.1, 127.0, 126.5, 125.3, 122.6, 122.1, 107.1, 106.1, 66.8, 56.2, 43.7, and 40.8. ESI-MS, $[M - H]^-$, m/z (au)/relative intensity (%): 425.9/100. $[M + H]^+$, m/z (au)/relative intensity (%): 427.9/100. +160.07 (c 0.0563, DMSO).

*(2-(6-(Benzothiazol-2-yl)-8-methoxy-3-oxo-2,3-dihydro-4H-benzo[1,4]oxazin-4-yl)acetyl)-L-alanine (**12b**).* Following the procedure for the synthesis of compound **7b**: a mixture of compound **11b** (2.28 g, 5 mmol), ethanol (5 mL), and 10% NaOH solution (10 mL) was heated to reflux for approximately 5 min. Recrystallization in ethanol: water (1:1, v/v) gave the product as a white solid (1.87 g, 85%): mp 294−296 °C. HRMS (ESI-TOF) m/z: $[M + H]^+$ calcd for $C_{21}H_{20}N_3O_6S$, 442.1067; found, 442.1055. ^1H NMR (DMSO-d_6, 600 MHz): δ (ppm) 8.68 (d, J = 7.8 Hz, 1H), 8.12 (d, J = 7.8 Hz, 1H), 8.04 (d, J = 7.8 Hz, 1H), 7.54 (dd, $J_1 = J_2$ = 7.8 Hz, 1H), 7.47 (s, 1H), 7.45 (d, J = 7.2 Hz, 1H), 7.19 (d, J = 1.2 Hz, 1H), 4.79 (s, 2H), 4.71 (d, J = 16.8 Hz, 1H), 4.64 (t, J = 13.8 Hz, 1H), 4.28 (td, J = 14.4, 6.6 Hz, 1H), 3.94 (s, 3H), and 1.33 (d, J = 7.2 Hz, 3H). ^{13}C NMR (DMSO-d_6, 150 MHz): δ (ppm) 173.6, 166.6, 166.0, 163.9, 153.3, 148.7, 136.4, 134.5, 130.1, 127.0, 126.5, 125.3, 122.6, 122.1, 106.9, 106.0, 66.8, 55.2, 47.6, 43.4, and 17.3. ESI-MS, $[M + H]^+$, m/z (au)/relative intensity (%): 442.1/100. $[M - H]^-$, m/z (au)/relative intensity (%): 440.1/100. −26.03 (c 0.1625, DMSO).

https://doi.org/10.1021/acsomega.4c06760
ACS Omega 2025, 10, 10835−10851

*(2-(6-(Benzothiazol-2-yl)-8-methoxy-3-oxo-2,3-dihydro-4H-benzo[1,4]oxazin-4-yl)acetyl)-L-valine (**12c**).* Following the procedure for the synthesis of compound **7c**: a mixture of compound **11c** (2.42 g, 5 mmol), ethanol (5 mL), and 10% NaOH solution (10 mL) was heated to reflux for approximately 5 min. Recrystallization in ethanol: water (1:1, v/v) gave the product as a white solid (2.04 g, 87%): mp 304–306 °C. HRMS (ESI-TOF) m/z: $[M + H]^+$ calcd for $C_{23}H_{24}N_3O_6S$, 470.1380; found, 470.1370. ^1H NMR (DMSO-d_6, 600 MHz): δ (ppm) 8.56 (d, J = 9.0 Hz, 1H), 8.11 (d, J = 7.8 Hz, 1H), 8.01 (d, J = 8.4 Hz, 1H), 7.55 (dd, J_1 = J_2 = 7.8 Hz, 1H), 7.45 (dd, J_1 = J_2 = 7.8 Hz, 1H), 7.44 (s, 1H), 7.23 (d, J = 1.2 Hz, 1H), 4.82 (d, J = 16.8 Hz, 1H), 4.79 (s, 2H), 4.68 (d, J = 16.2 Hz, 1H), 4.23 (q, J = 5.4 Hz, 1H), 3.94 (s, 3H), 2.11 (q, J = 6.6 Hz, 1H), 0.93 (d, J = 6.6 Hz, 3H), and 0.89 (d, J = 6.6 Hz, 3H). ^{13}C NMR (DMSO-d_6, 150 MHz): δ (ppm) 172.6, 166.5, 166.4, 163.9, 153.3, 148.7, 136.4, 134.4, 130.1, 127.0, 126.6, 125.3, 122.5, 122.1, 106.6, 106.2, 66.8, 57.2, 56.2, 43.2, 30.0, 19.1, and 17.8. ESI-MS, $[M + H]^+$, m/z (au)/relative intensity (%): 470.0/100. $[M - H]^-$, m/z (au)/relative intensity (%): 468.0/100. −45.28 (c 0.0625, MeOH).

*(2-(6-(Benzothiazol-2-yl)-8-methoxy-3-oxo-2,3-dihydro-4H-benzo[1,4]oxazin-4-yl)acetyl)-L-leucine (**12d**).* Following the procedure for the synthesis of compound **7d**: a mixture of compound **11d** (2.49 g, 5 mmol), ethanol (5 mL), and 10% NaOH solution (10 mL) was heated to reflux for approximately 5 min. Recrystallization in ethanol/water (1:1, v/v) gave the product as a white solid (2.08 g, yield 86%): mp 311–313 °C. HRMS (ESI-TOF) m/z: $[M + H]^+$ calcd for $C_{24}H_{26}N_3O_6S$, 484.1537; found, 484.1513. ^1H NMR (DMSO-d_6, 600 MHz): δ (ppm) 8.63 (d, J = 8.4 Hz, 1H), 8.11 (d, J = 8.4 Hz, 1H), 8.03 (d, J = 8.4 Hz, 1H), 7.55 (dd, J_1 = J_2 = 7.8 Hz, 1H), 7.46 (dd, J_1 = J_2 = 7.8 Hz, 1H), 7.45 (s, 1H), 7.17 (s, 1H), 4.80 (s, 2H), 4.75 (d, J = 18.0 Hz, 1H),4.62 (d, J = 16.8 Hz, 1H), 1.55–1.62 (m, 2H), 1.48–1.51 (m, 1H), 0.76 (d, J = 6.6 Hz, 3H), and 0.67 (d, J = 6.0 Hz, 3H). ^{13}C NMR (DMSO-d_6, 150 MHz): δ (ppm) 173.6, 166.6, 166.2, 163.8, 153.4, 148.7, 136.5, 134.5, 130.0, 127.0, 126.5, 125.3, 122.6, 122.1, 106.7, 106.2, 66.8, 56.2, 50.1, 43.2, 24.1, 22.8, and 20.8. −46.63 (c 0.1313, MeOH).

*(2-(6-(Benzothiazol-2-yl)-8-methoxy-3-oxo-2,3-dihydro-4H-benzo[1,4]oxazin-4-yl)acetyl)-L-alloisoleucine (**12e**).* Following the procedure for the synthesis of compound **7e**: a mixture of compound **11e** (2.49 g, 5 mmol), ethanol (5 mL), and 10% NaOH solution (10 mL) was heated to reflux for approximately 5 min. Recrystallization in ethanol: water (1:1, v/v) gave the product as a white solid (2.17 g, yield 90%): mp 314–316 °C. HRMS (ESI-TOF) m/z: $[M + H]^+$ calcd for $C_{24}H_{26}N_3O_6S$, 484.1537; found, 484.1520. ^1H NMR (DMSO-d_6, 600 MHz): δ (ppm) 12.70 (s, 1H), 8.57 (d, J = 5.4 Hz, 1H), 8.11 (d, J = 7.8 Hz, 1H), 8.02 (d, J = 8.4 Hz, 1H), 7.55 (ddd, J_1 = 1.2 Hz, J_2 = J_3 = 7.8 Hz, 1H), 7.46 (ddd, J_1 = 1.2 Hz, J_2 = J_3 = 8.4 Hz, 1H), 7.44 (d, J = 1.8, 1H), 7.21 (d, J = 1.8 Hz, 1H), 4.81 (d, J = 16.8 Hz, 1H), 4.78 (s, 2H), 4.65 (d, J = 13.2 Hz, 1), 4.24 (q, J = 6.0, 1H), 3.94 (s, 3H), 1.81–1.83 (m, 1H), 1.40–1.43 (m, 1H), 1.21–1.25 (m, 2H), 0.85 (d, J = 6.6 Hz, 3H), and 0.77 (t, J = 7.2 Hz, 3H). ^{13}C NMR (DMSO-d_6, 150 MHz): δ (ppm) 172.6, 166.5, 166.3, 163.9, 153.3, 148.7, 136.4, 134.4, 130.0, 127.0, 126.5, 125.3, 122.5, 122.1, 106.6, 106.2, 66.8, 56.3, 56.2, 43.1, 36.5, 24.2, 15.5, and 11.1. ESI-MS, $[M + H]^+$, m/z (au)/relative intensity (%): 484.0/100. $[M - H]^-$, m/z (au)/relative intensity (%): 481.9/100. −40.38 (c 0.1313, MeOH).

*(2-(6-(Benzothiazol-2-yl)-8-methoxy-3-oxo-2,3-dihydro-4H-benzo[1,4]oxazin-4-yl)acetyl)-L-phenylalanine (**12f**).* Following the procedure for the synthesis of compound **7f**: a mixture of compound **11f** (2.66 g, 5 mmol), ethanol (5 mL), and 10% NaOH solution (10 mL) was heated to reflux for approximately 5 min. Recrystallization in ethanol/water (1:1, v/v) gave the product as a white solid (2.1 g, yield 81%): mp 310–311 °C. HRMS (ESI-TOF) m/z: $[M + H]^+$ calcd for $C_{27}H_{24}N_3O_6S$, 518.1380; found, 518.1372. ^1H NMR (DMSO-d_6, 600 MHz): δ (ppm) 12.80 (s, 1H), 8.66 (d, J = 8.4 Hz, 1H), 8.12 (d, J = 8.4 Hz, 1H), 8.03 (d, J = 8.4 Hz, 1H), 7.52–7.56 (m, 1H), 7.45–7.47 (m, 2H), 7.15–7.24 (m, 4H), 7.12 (d, J = 1.8 Hz, 1H), 7.08 (t, J = 7.2 Hz, 1H), 4.78 (d, J = 1.8 Hz, 2H), 4.63 (s, 2H), 4.47 (td, J = 4.8, 7.8 Hz, 1H), 3.94 (s, 3H), 3.07 (dd, J = 4.8, 13.8 Hz, 1H), and 2.94 (dd, J = 8.4, 13.2 Hz, 1H). ^{13}C NMR (DMSO-d_6, 150 MHz): δ (ppm) 172.4, 166.7, 166.9, 163.9, 153.4, 148.7, 137.3, 136.4, 134.5, 130.0, 128.9, 128.0, 127.0, 126.5, 126.2, 125.3, 122.6, 122.1, 106.8, 106.1, 66.8, 56.2, 53.6, 43.4, and 36.7. ESI-MS, $[M + H]^+$, m/z (au)/relative intensity (%): 518.0/100. $[M - H]^-$, m/z (au)/relative intensity (%): 518.0/100. +46.81 (c 0.0437, DMSO).

Molecular Docking and MD. The structures of the tested compounds were drawn using the ChemSketch software, then optimized and energy minimized with the MMFF94s force field in Avogadro software.[53,59] The optimized compounds were prepared for molecular docking using AutoDockTools. The three-dimensional structure of the target protein, human AChE, was obtained from the Protein Data Bank (PDB) (http://www.rcsb.org) with PDB ID 4EY7.[60] Receptor preparation involved the removal of heteroatoms (water and ions), the addition of polar hydrogens, and assigning charges. Active sites were identified by setting grid boxes around constrained ligand molecules. Docking studies were conducted using AutoDock Vina v1.2.3, and Discovery Studio Visualizer software was used for visualization.[57,61] Subsequently, MD simulations were performed with GROMACS v2023, running a 200 ns production phase.[58] Parameter and topology files were prepared as previously reported.[62] System equilibration was achieved through *NVT* and *NPT* ensembles after solvation with water molecules and neutralization with counterions. GROMACS tools were then used to analyze trajectory files, calculating rmsd values to assess the dynamic behavior of the protein–ligand complex and the impact of ligand binding on the protein structure and stability. Graphical representations were created with XMGRACE software.

Biological Activity. The synthesized benzothiazole and benzoxazine derivatives were evaluated for in vitro enzyme AChE inhibition activity, and donepezil was used as a standard.

In Vitro AChE Inhibition Activity. This experiment is based on the theory that Alzheimer's patients experience a significant decrease in the neurotransmitter acetylcholine (ACh), which impacts their cognitive abilities. Consequently, substances that inhibit AChE—the enzyme responsible for hydrolyzing ACh into choline and acetic acid—can increase ACh concentration and prolong its activity at nerve synapses, thereby alleviating patient symptoms. The AChE inhibition assay is conducted using Ellman's method, developed by Ellman and colleagues in 1961. This method relies on the hydrolysis of acetylthiocholine by AChE to produce thiocholine, which reacts with the reagent 5,5′-dithiobis-2-nitrobenzoic acid (DTNB) to form the yellow compound 5-thio-2-nitrobenzoic acid. The amount of this colored product, which is proportional to AChE activity, can be measured at 412 nm to assess AChE inhibition activity by the test sample. The experiment is structured as follows: prepare 96-well plates with a total volume of 200 μL per well. Sequentially add Tris-HCl buffer solution (pH = 8), the test sample, and enzyme solution 0.25 IU/mL to each well. Mix thoroughly and incubate for 15 min at 25 °C. Then add DTNB reagent solution 2.4 mM and ATCI solution 2.4 mM to the wells, mix well, and continue incubating for another 15 min at 25 °C. Measure the optical absorption at 412 nm, performing three replicates for accuracy, and use donepezil as the standard compound.[63−65]

■ CONCLUSIONS

Benzothiazole and benzo[1,4]oxazin-3(4*H*)-one derivatives were successfully synthesized from vanillin via a straightforward and cost-effective procedure. The synthesis process involves simple reactions with inexpensive reagents, yielding 21 different derivatives with yields ranging from 72% to 95%. Notably, six derivatives containing both the benzothiazole and benzo[1,4]oxazin-3(4*H*)-one scaffolds were synthesized using a similar method, omitting purification prior to hydrolysis. This highlights the essential role of the coupling agent HATU in this reaction with a proposed mechanism involving an α-lactam intermediate and a Favorskii-like rearrangement. Additionally, theoretical calculations based on the DFT method suggest that the energy barriers can be overcome by the energy generated from the exothermic reaction, making the formation of these derivatives, particularly structure **II**, thermodynamically feasible. The synthesized derivatives were evaluated for in vitro AChE inhibition activity. Compounds **6d** and **6f** demonstrated significant activity, with IC_{50} values between 25.33 and 32 μg/mL, compared to donepezil with an IC_{50} of 0.028 μg/mL. Molecular docking studies align with the experimental results, revealing key binding interactions (hydrogen bonds, pi−pi, and pi−alkyl interactions) with important amino acid residues. Furthermore, MD simulations indicate high structural stability, especially for compound **6f**, supporting the potential of this scaffold for AD treatment and warranting further development.

■ ASSOCIATED CONTENT

Supporting Information

The Supporting Information is available free of charge at https://pubs.acs.org/doi/10.1021/acsomega.4c06760.

Extended information on the quantum chemical characterizations (PDF)

■ AUTHOR INFORMATION

Corresponding Author

Hoan Quoc Duong − *Faculty of Chemistry, Hanoi National University of Education, Hanoi 100000, Vietnam;* orcid.org/0000-0001-7540-6142; Email: hoandq@hnue.edu.vn

Authors

Du Duc Nguyen − *Faculty of Chemistry, Hanoi National University of Education, Hanoi 100000, Vietnam*

Dat Van Nguyen − *Faculty of Chemistry, Hanoi National University of Education, Hanoi 100000, Vietnam;* orcid.org/0009-0007-4623-6819

Hue Van Nguyen − *Faculty of Chemistry and Center for Computational Science, Hanoi National University of Education, Hanoi 100000, Vietnam*

Giang Huong Thi Vu − *Faculty of Chemistry and Center for Computational Science, Hanoi National University of Education, Hanoi 100000, Vietnam*

Ha Xuan Nguyen − *Institute of Natural Products Chemistry, Vietnam Academy of Science and Technology, Hanoi 100000, VietNam*

Hai Hong Thi Le − *Faculty of Chemistry, Hanoi National University of Education, Hanoi 100000, Vietnam; Institute of Natural Science, Hanoi National University of Education, Hanoi 100000, Vietnam;* orcid.org/0000-0002-3157-6980

Dien Huu Pham − *Faculty of Chemistry, Hanoi National University of Education, Hanoi 100000, Vietnam;* orcid.org/0009-0004-2799-4401

Trang Ha Thi Nguyen − *Faculty of Chemistry, Hanoi National University of Education, Hanoi 100000, Vietnam*

Tai Minh Trinh − *Faculty of Chemistry, Hanoi National University of Education, Hanoi 100000, Vietnam*

Nga Thuy Nguyen − *Faculty of Chemistry, Hanoi National University of Education, Hanoi 100000, Vietnam;* orcid.org/0009-0008-5008-7083

Hue Minh Thi Nguyen − *Faculty of Chemistry and Center for Computational Science and Institute of Natural Science, Hanoi National University of Education, Hanoi 100000, Vietnam;* orcid.org/0000-0001-6373-4691

Complete contact information is available at: https://pubs.acs.org/10.1021/acsomega.4c06760

Author Contributions

All authors contributed to the conceptualization and realization of the study. Du Duc Nguyen and Dat Van Nguyen wrote the first draft; Hue Van Nguyen, Giang Huong Thi Vu, Ha Xuan Nguyen, Trang Ha Thi Pham, Tai Minh Trinh, and Nga Thuy Nguyen did investigation and calculations. Hai Hong Thi Le, Dien Huu Pham, and Hue Minh Thi Nguyen analyzed results and revised the manuscript. Hoan Quoc Duong supervised, interpreted the data, and revised the manuscript.

Notes

The authors declare no competing financial interest.

■ ACKNOWLEDGMENTS

This research is supported by The Ministry of Education and Training of Vietnam under the project code B2023-SPH-16.

■ REFERENCES

(1) Ali, R.; Siddiqui, N. Biological Aspects of Emerging Benzothiazoles: A Short Review. *J. Chem.* **2013**, *2013*, 345198.

(2) Leleu-Chavain, N.; Baudelet, D.; Heloire, V. M.; Rocha, D. E.; Renault, N.; Barczyk, A.; Djouina, M.; Body-Malapel, M.; Carato, P.; Millet, R. Benzo[d]Thiazol-2(3H)-Ones as New Potent Selective CB(2) Agonists with Anti-Inflammatory Properties. *Eur. J. Med. Chem.* **2019**, *165*, 347−362.

(3) Cindrić, M.; Perić, M.; Kralj, M.; Martin-Kleiner, I.; David-Cordonnier, M.-H.; Paljetak, H. Č.; Matijašić, M.; Verbanac, D.; Karminski-Zamola, G.; Hranjec, M. Antibacterial and Antiproliferative Activity of Novel 2-Benzimidazolyl- and 2-Benzothiazolyl-Substituted Benzo[b]Thieno-2-Carboxamides. *Mol. Divers.* **2018**, *22* (3), 637−646.

(4) Akhtar, T.; Hameed, S.; Al-Masoudi, N. A.; Loddo, R.; Colla, P. L. In Vitro Antitumor and Antiviral Activities of New Benzothiazole and 1,3,4-Oxadiazole-2-Thione Derivatives. *Acta Pharm.* **2008**, *58* (2), 135−149.

(5) Nagararaju, G.; Sai, K. B.; Chandana, K.; Gudipati, M.; Suresh, P. V.; Ramarao, N. Synthesis, Evaluation of Antioxidant and Antimicrobial Study of 2-Substituted Benzothiazole Derivatives. *Indo Am. J. Pharm. Res.* **2015**, *50* (03), 1288−1296.

(6) Khan, K. M.; Mesaik, M. A.; Abdalla, O. M.; Rahim, F.; Soomro, S.; Halim, S. A.; Mustafa, G.; Ambreen, N.; Khalid, A. S.; Taha, M.; Perveen, S.; Alam, M. T.; Hameed, A.; Ul-Haq, Z.; Ullah, H.; Rehman, Z. U.; Siddiqui, R. A.; Voelter, W. The Immunomodulation Potential of the Synthetic Derivatives of Benzothiazoles: Implications in Immune System Disorders through in Vitro and in Silico Studies. *Bioorg. Chem.* **2016**, *64*, 21−28.

(7) Weekes, A. A.; Westwell, A. D. 2-Arylbenzothiazole as a Privileged Scaffold in Drug Discovery. *Curr. Med. Chem.* **2009**, *16* (19), 2430−2440.

(8) Zengin, M.; Unsal-Tan, O.; Küçükkılınç, T. T.; Ayazgok, B.; Balkan, A. Design and Synthesis of 2-Substitutedphenyl Benzo[d]-Thiazole Derivatives and Their *β*-Amyloid Aggregation and Cholinesterase Inhibitory Activities. *Pharm. Chem. J.* **2019**, *53*, 322−328.

(9) Palmer, P. J.; Trigg, R. B.; Warrington, J. V. Benzothiazolines as Antituberculous Agents. *J. Med. Chem.* **1971**, *14* (3), 248−251.

(10) Huang, Q.; Mao, J.; Wan, B.; Wang, Y.; Brun, R.; Franzblau, S. G.; Kozikowski, A. P. Searching for New Cures for Tuberculosis: Design, Synthesis, and Biological Evaluation of 2-Methylbenzothiazoles. *J. Med. Chem.* **2009**, *52* (21), 6757−6767.

(11) Burger, A.; Sawhney, S. N. Antimalarials. 3. Benzothiazole Amino Alcohols. *J. Med. Chem.* **1968**, *11* (2), 270−273.

(12) Moreno-Díaz, H.; Villalobos-Molina, R.; Ortiz-Andrade, R.; Díaz-Coutiño, D.; Medina-Franco, J. L.; Webster, S. P.; Binnie, M.; Estrada-Soto, S.; Ibarra-Barajas, M.; León-Rivera, I.; Navarrete-Vázquez, G. Antidiabetic Activity of N-(6-Substituted-1,3-Benzothiazol-2-Yl)Benzenesulfonamides. *Bioorg. Med. Chem. Lett.* **2008**, *18* (9), 2871−2877.

(13) Watanabe, H.; Ono, M.; Ariyoshi, T.; Katayanagi, R.; Saji, H. Novel Benzothiazole Derivatives as Fluorescent Probes for Detection of *β*-Amyloid and *α*-Synuclein Aggregates. *ACS Chem. Neurosci.* **2017**, *8* (8), 1656−1662.

(14) Wu, Y.; Peng, X.; Fan, J.; Gao, S.; Tian, M.; Zhao, J.; Sun, S. Fluorescence Sensing of Anions Based on Inhibition of Excited-State Intramolecular Proton Transfer. *J. Org. Chem.* **2007**, *72* (1), 62−70.

(15) Bravo, H. R.; Lazo, W. Antialgal and Antifungal Activity of Natural Hydroxamic Acids and Related Compounds. *J. Agric. Food Chem.* **1996**, *44* (6), 1569−1571.

(16) Brown, K. S.; Djerassi, C. Alkaloid Studies. XLVI.1 The Alkaloids of Aspidosperma Obscurinervium Azembuja. A New Class of Heptacyclic Indole Alkaloids2. *J. Am. Chem. Soc.* **1964**, *86* (12), 2451−2463.

(17) Sicker, D.; Schulz, M. Benzoxazinones in Plants: Occurrence, Synthetic Access, and Biological Activity. In *Bioactive Natural Products (Part H)*; Atta-ur-Rahman, B. T.-S., N, P. C., Eds.; Elsevier, 2002; Vol. *27*, pp 185−232.

(18) Matsuoka, H.; Ohi, N.; Mihara, M.; Suzuki, H.; Miyamoto, K.; Maruyama, N.; Tsuji, K.; Kato, N.; Akimoto, T.; Takeda, Y.; Yano, K.; Kuroki, T. Antirheumatic Agents: Novel Methotrexate Derivatives Bearing a Benzoxazine or Benzothiazine Moiety. *J. Med. Chem.* **1997**, *40* (1), 105−111.

(19) Largeron, M.; Lockhart, B.; Pfeiffer, B.; Fleury, M.-B. Synthesis and in Vitro Evaluation of New 8-Amino-1,4-Benzoxazine Derivatives as Neuroprotective Antioxidants. *J. Med. Chem.* **1999**, *42* (24), 5043−5052.

(20) Jiao, P.-F.; Zhao, B.-X.; Wang, W.-W.; He, Q.-X.; Wan, M.-S.; Shin, D.-S.; Miao, J.-Y. Design, Synthesis, and Preliminary Biological Evaluation of 2,3-Dihydro-3-Hydroxymethyl-1,4-Benzoxazine Derivatives. *Bioorg. Med. Chem. Lett.* **2006**, *16* (11), 2862−2867.

(21) Touzeau, F.; Arrault, A.; Guillaumet, G.; Scalbert, E.; Pfeiffer, B.; Rettori, M.-C.; Renard, P.; Mérour, J.-Y. Synthesis and Biological Evaluation of New 2-(4,5-Dihydro-1H-Imidazole-2-Yl)-3,4-Dihydro-2H-1,4-Benzoxazine Derivatives. *J. Med. Chem.* **2003**, *46* (10), 1962−1979.

(22) Varshney, H.; Ahmad, A.; Rauf, A.; Husain, F. M.; Ahmad, I. Synthesis and Antimicrobial Evaluation of Fatty Chain Substituted 2,5-Dimethyl Pyrrole and 1,3-Benzoxazin-4-One Derivatives. *J. Saudi Chem. Soc.* **2017**, *21*, S394−S402.

(23) Králová, P.; Ručilová, V.; Soural, M. Polymer-Supported Syntheses of Heterocycles Bearing Oxazine and Thiazine Scaffolds. *ACS Comb. Sci.* **2018**, *20* (9), 529−543.

(24) Jung, C.; Müller, B. K.; Lamb, D. C.; Nolde, F.; Müllen, K.; Bräuchle, C. A New Photostable Terrylene Diimide Dye for Applications in Single Molecule Studies and Membrane Labeling. *J. Am. Chem. Soc.* **2006**, *128* (15), 5283−5291.

(25) Zvěřová, M. Clinical aspects of Alzheimer's disease. *Clin. Biochem.* **2019**, *72*, 3−6.

(26) Liu, T.; Chen, S.; Du, J.; Xing, S.; Li, R.; Li, Z. Design, Synthesis, and Biological Evaluation of Novel (4-(1,2,4-Oxadiazol-5-Yl)Phenyl)-2-Aminoacetamide Derivatives as Multifunctional Agents for the Treatment of Alzheimer's Disease. *Eur. J. Med. Chem.* **2022**, *227*, 113973.

(27) Saeedi, M.; Mehranfar, F. Challenges and approaches of drugs such as memantine, donepezil, rivastigmine, and aducanumab in the treatment, control and management of Alzheimer's disease. *Recent Pat. Biotechnol.* **2022**, *16* (2), 102−121.

(28) Hafez, D. E.; Dubiel, M.; La Spada, G.; Catto, M.; Reiner-Link, D.; Syu, Y.-T.; Abdel-Halim, M.; Hwang, T.-L.; Stark, H.; Abadi, A. H. Novel Benzothiazole Derivatives as Multitargeted-Directed Ligands for the Treatment of Alzheimer's Disease. *J. Enzyme Inhib. Med. Chem.* **2023**, *38* (1), 2175821.

(29) Turan-Zitouni, G.; Hussein, W.; Saglik, N. B.; Baysal, M.; Kaplancikli, A. Z. Fighting Against Alzheimer'sDisease: Synthesis of New Pyrazoline and Benzothiazole Derivatives as New Acetylcholinesterase and MAO Inhibitors. *Lett. Drug Des. Discovery* **2018**, *15*, 414−427.

(30) Mallesh, R.; Khan, J.; Pradhan, K.; Roy, R.; Jana, N. R.; Jaisankar, P.; Ghosh, S. Design and Development of Benzothiazole-Based Fluorescent Probes for Selective Detection of A*β* Aggregates in Alzheimer's Disease. *ACS Chem. Neurosci.* **2022**, *13* (16), 2503−2516.

(31) Wang, L.; Ankati, H.; Akubathini, S. K.; Balderamos, M.; Storey, C. A.; Patel, A. V.; Price, V.; Kretzschmar, D.; Biehl, E. R.; D'Mello, S. R. Identification of Novel 1,4-Benzoxazine Compounds That Are Protective in Tissue Culture and in Vivo Models of Neurodegeneration. *J. Neurosci. Res.* **2010**, *88* (9), 1970−1984.

(32) Mortimer, C. G.; Wells, G.; Crochard, J.-P.; Stone, E. L.; Bradshaw, T. D.; Stevens, M. F. G.; Westwell, A. D. Antitumor Benzothiazoles. 26. 2-(3,4-Dimethoxyphenyl)-5-Fluorobenzothiazole (GW 610, NSC 721648), a Simple Fluorinated 2-Arylbenzothiazole, Shows Potent and Selective Inhibitory Activity against Lung, Colon, and Breast Cancer Cell Lines. *J. Med. Chem.* **2006**, *49* (1), 179−185.

(33) Maleki, B.; Salehabadi, H. Ammonium Chloride; as a Mild and Efficient Catalyst for the Synthesis of Some 2-Arylbenzothiazoles and Bisbenzothiazole Derivatives. *Eur. J. Chem.* **2010**, *1* (4), 377−380.

(34) Batista, R. M. F.; Costa, S. P. G.; Raposo, M. M. M. Synthesis of New Fluorescent 2-(2′,2″-Bithienyl)-1,3-Benzothiazoles. *Tetrahedron Lett.* **2004**, *45* (13), 2825−2828.

(35) Pandey, A. M.; Mondal, S.; Gnanaprakasam, B. Continuous-Flow Direct Azidation of Alcohols and Peroxides for the Synthesis of Quinoxalinone, Benzooxazinone, and Triazole Derivatives. *J. Org. Chem.* **2022**, *87* (15), 9926−9939.

(36) Zheng, B.-F.; Zuo, Y.; Huang, G.-Y.; Wang, Z.-Z.; Ma, J.-Y.; Wu, Q.-Y.; Yang, G.-F. Synthesis and Biological Activity Evaluation of Benzoxazinone-Pyrimidinedione Hybrids as Potent Protoporphyrinogen IX Oxidase Inhibitor. *J. Agric. Food Chem.* **2023**, *71* (39), 14221−14231.

(37) Segura-Quezada, L. A.; Torres-Carbajal, K. R.; Mali, N.; Patil, D. B.; Luna-Chagolla, M.; Ortiz-Alvarado, R.; Tapia-Juárez, M.;

Fraire-Soto, I.; Araujo-Huitrado, J. G.; Granados-López, A. J.; Gutiérrez-Hernández, R.; Reyes-Estrada, C. A.; López-Hernández, Y.; López, J. A.; Chacón-García, L.; Solorio-Alvarado, C. R. Gold(I)-Catalyzed Synthesis of 4H-Benzo[d][1,3]oxazines and Biological Evaluation of Activity in Breast Cancer Cells. *ACS Omega* **2022**, *7* (8), 6944−6955.

(38) Gali, S.; Raghu, D.; Mallikanti, V.; Thumma, V.; Vaddiraju, N. Design, synthesis of benzimidazole tethered 3,4-dihydro-2H-benzo[e][1, 3] oxazines as anticancer agents. *Mol. Diversity* **2024**, *28*, 1347−1361.

(39) Mai, T. N. N.; Hoan, Q. D.; Tuyet, T. A. V.; Thu Trang, T. T.; Linh, K. D.; Huan, T. T. An Effective Assembling of Novel Derivatives Containing Both Benzo[d]Thiazole and Benzo[d]Oxazole Rings. *Lett. Org. Chem.* **2020**, *17* (11), 815−822.

(40) Shitha, G.; Amma, V. K.; Babu, g.; Biju, c. R. In-silico docking investigation, synthesis and invitro anticancer study of benzoxazole derivatives. *J. Drug Deliv. Therapeut.* **2014**, *4* (6), 1014.

(41) Han, S.-Y.; Kim, Y.-A. Recent Development of Peptide Coupling Reagents in Organic Synthesis. *Tetrahedron* **2004**, *60* (11), 2447−2467.

(42) Garg, A.; Borah, D.; Trivedi, P.; Gogoi, D.; Chaliha, A. K.; Ali, A. A.; Chetia, D.; Chaturvedi, V.; Sarma, D. A. Simple Work-Up-Free, Solvent-Free Approach to Novel Amino Acid Linked 1,4-Disubstituted 1,2,3-Triazoles as Potent Antituberculosis Agents. *ACS Omega* **2020**, *5* (46), 29830−29837.

(43) Balakrishna, R. B.; Gopisetti, J. M. Synthesis of 2-(3-Oxo-2, 3-Dihydro-4H-Benzo [b] [1,4] Oxazin - 4 -Yl) - N -Substituted Phenylacetamides. *Futur. J. Pharm. Heal. Sci.* **2022**, *2* (2 SE-Original Articles), 95−101.

(44) Baumgarten, H. E.; Zey, R. L.; Krolls, U. Reactions of amines. Ix. The rearrangement of n-t-butyl-n-chloroamides1−2. *J. Am. Chem. Soc.* **1961**, *83* (21), 4469−4470.

(45) Guijarro, D.; Yus, M. The Favorskii Rearrangement: Synthetic Applications. *Curr. Org. Chem.* **2005**, *9*, 1713−1735.

(46) Becke, A. D. Density Functional Thermochemistry. I. The Effect of the Exchange Only Gradient Correction. *J. Chem. Phys.* **1992**, *96* (3), 2155−2160.

(47) Cao, X.; Dolg, M. Valence Basis Sets for Relativistic Energy-Consistent Small-Core Lanthanide Pseudopotentials. *J. Chem. Phys.* **2001**, *115* (16), 7348−7355.

(48) Mardirossian, N.; Head-Gordon, M. Thirty Years of Density Functional Theory in Computational Chemistry: An Overview and Extensive Assessment of 200 Density Functionals. *Mol. Phys.* **2017**, *115* (19), 2315−2372.

(49) Johnson, E. R.; Keinan, S.; Mori-Sánchez, P.; Contreras-García, J.; Cohen, A. J.; Yang, W. Revealing Noncovalent Interactions. *J. Am. Chem. Soc.* **2010**, *132* (18), 6498−6506.

(50) Lu, T.; Chen, F. M. Multiwfn: A multifunctional wavefunction analyzer. *J. Comput. Chem.* **2012**, *33* (5), 580−592.

(51) Espinosa, E.; Molins, E.; Lecomte, C. Hydrogen Bond Strengths Revealed by Topological Analyses of Experimentally Observed Electron Densities. *Chem. Phys. Lett.* **1998**, *285* (3), 170−173.

(52) Luque, F. J.; Muñoz-Torrero, D. Acetylcholinesterase: A Versatile Template to Coin Potent Modulators of Multiple Therapeutic Targets. *Acc. Chem. Res.* **2024**, *57* (4), 450−467.

(53) Peitzika, S.-C.; Pontiki, E. A Review on Recent Approaches on Molecular Docking Studies of Novel Compounds Targeting Acetylcholinesterase in Alzheimer Disease. *Molecules* **2023**, *28* (3), 1084.

(54) Liu, K.; Kokubo, H. Exploring the Stability of Ligand Binding Modes to Proteins by Molecular Dynamics Simulations: A Cross-Docking Study. *J. Chem. Inf. Model.* **2017**, *57* (10), 2514−2522.

(55) Frisch, M.; Trucks, G.; Schlegel, H.; Scuseria, G.; Robb, M.; Cheeseman, J.; Scalmani, G.; Barone, V.; Mennucci, B.; Petersson, G.; Nakatsuji, H.; Caricato, M.; Li, X.; Hratchian, H.; Izmaylov, A.; Bloino, J.; Zheng, G.; Sonnenberg, J.; Hada, M.; Fox, D. *Gaussian 09*, 2009.

(56) Humphrey, W.; Dalke, A.; Schulten, K. VMD: Visual Molecular Dynamics. *J. Mol. Graph.* **1996**, *14* (1), 33−38.

(57) Eberhardt, J.; Santos-Martins, D.; Tillack, A. F.; Forli, S. AutoDock Vina 1.2.0: New Docking Methods, Expanded Force Field, and Python Bindings. *J. Chem. Inf. Model.* **2021**, *61* (8), 3891−3898.

(58) Van Der Spoel, D.; Lindahl, E.; Hess, B.; Groenhof, G.; Mark, A. E.; Berendsen, H. J. C. GROMACS: Fast, Flexible, and Free. *J. Comput. Chem.* **2005**, *26* (16), 1701−1718.

(59) Kosar, B.; Albayrak, C. Spectroscopic Investigations and Quantum Chemical Computational Study of (E)-4-Methoxy-2-[(p-Tolylimino)Methyl]Phenol. *Spectrochim. Acta, Part A* **2011**, *78* (1), 160−167.

(60) Cheung, J.; Rudolph, M. J.; Burshteyn, F.; Cassidy, M. S.; Gary, E. N.; Love, J.; Franklin, M. C.; Height, J. J. Structures of Human Acetylcholinesterase in Complex with Pharmacologically Important Ligands. *J. Med. Chem.* **2012**, *55* (22), 10282−10286.

(61) Trott, O.; Olson, A. J. AutoDock Vina: Improving the Speed and Accuracy of Docking with a New Scoring Function, Efficient Optimization, and Multithreading. *J. Comput. Chem.* **2010**, *31* (2), 455−461.

(62) Le, V. T. T.; Hung, H. V.; Ha, N. X.; Le, C. H.; Minh, P. T.; Lam, D. T. Natural Phosphodiesterase-4 Inhibitors with Potential Anti-Inflammatory Activities from Millettia Dielsiana. *Molecules* **2023**, *28*, 7253.

(63) Somani, G.; Kulkarni, C.; Shinde, P.; Shelke, R.; Laddha, K.; Sathaye, S. In Vitro Acetylcholinesterase Inhibition by Psoralen Using Molecular Docking and Enzymatic Studies. *J. Pharm. BioAllied Sci.* **2015**, *7* (1), 32−36.

(64) Min, B. S.; Cuong, T. D.; Lee, J.-S.; Shin, B.-S.; Woo, M. H.; Hung, T. M. Cholinesterase Inhibitors from Cleistocalyx Operculatus Buds. *Arch. Pharm. Res.* **2010**, *33* (10), 1665−1670.

(65) Ellman, G. L.; Courtney, K. D.; Andres, V. J.; Feather-Stone, R. M. A New and Rapid Colorimetric Determination of Acetylcholinesterase Activity. *Biochem. Pharmacol.* **1961**, *7*, 88.

https://doi.org/10.1021/acsomega.4c06760
ACS Omega 2025, 10, 10835−10851